

Radiogenic Isotopic Characterization and Petrogenesis of Host Rocks to the Greens Creek Deposit

By Wayne R. Premo and Cliff D. Taylor

Chapter 12 of

Geology, Geochemistry, and Genesis of the Greens Creek Massive Sulfide Deposit, Admiralty Island, Southeastern Alaska

Edited by Cliff D. Taylor and Craig A. Johnson

Professional Paper 1763

**U.S. Department of the Interior
U.S. Geological Survey**

Contents

Abstract.....	339
Introduction.....	339
Geology.....	341
Sampling.....	346
Results	347
Degree of Stability of the Isotopic Systematics	347
Initial Lead, Strontium, and Neodymium Isotopic Systematics of Greens Creek Host-Rock Lithologies.....	352
Metabasalts.....	354
Metagabbros	355
Phyllites	356
Argillites.....	358
Serpentinites.....	358
Crosscutting Diabases — Diorites	359
Discussion.....	359
Geologic Framework at Greens Creek	359
Petrotectonic Environment of the Greens Creek VMS Deposit	360
Initial Lead Isotopes of Greens Creek Host Rocks Compared to Ore Lead Compositions.....	360
Summary.....	363
Acknowledgments.....	363
References.....	363

Figures

1. Generalized map of terranes boundaries (bold lines) and major volcanogenic massive sulfide prospects southeast Alaska, showing the locations of the Late Triassic-age VMS deposits, including Greens Creek (#10), Pyrola (#11), and Gambier Bay (#19) on Admiralty Island.....	340
2. $^{206}\text{Pb}/^{204}\text{Pb} - ^{207}\text{Pb}/^{204}\text{Pb}$ correlation diagram showing the distribution of lead isotopic compositions (fields) for Alaskan volcanogenic massive sulfide (VMS) occurrences compared to model lead evolution curves (“upper crust,” “orogene,” and “depleted mantle”)	342
3. Simplified geologic map of Admiralty Island, showing locations for Greens Creek and Pyrola deposits, Gambier Bay, Windfall Harbor, the Mansfield Peninsula, and Staunch Point.....	343
4. Stratigraphy of the Greens Creek section, Admiralty Island, showing the orebody at the contact between footwall phyllites and hanging-wall argillites	344
5. Map of surface sampling sites at and near Greens Creek mine, Admiralty Island	345
6. (A) Geologic cross section, Greens Creek mine.....	346
6. (B) Predeformation, cross-sectional model, Greens Creek deposit, based on drill-core logging and underground and surface mapping.....	347

7. (A) Plot of uranium (U) concentration versus calculated initial $^{206}\text{Pb}/^{204}\text{Pb}$ at 215 Ma for whole-rock analyses of major Greens Creek host rocks, illustrating the possible isotopic disturbance of some whole-rock samples, probably during alteration.....	348
8. A comparison of calculated initial $^{206}\text{Pb}/^{204}\text{Pb}$ versus initial ϵ_{Nd} for whole-rock analyses from Greens Creek host rocks at 90 Ma	350
9. A comparison of the samarium-neodymium isotopic systematics of Greens Creek host rocks to Hyd Group metabasalt and Gallagher Ridge metagabbro isochrons, showing the extent of isotopic stability or variation within the different lithologic units.....	352
10. Pb-Pb correlation diagram ($^{206}\text{Pb}/^{204}\text{Pb}$ versus $^{207}\text{Pb}/^{204}\text{Pb}$) showing the distribution of initial lead compositions of Greens Creek host rocks relative to model lead evolution curves and fields for modern petrotectonic environments.....	353
11. Pb-Pb correlation diagram ($^{206}\text{Pb}/^{204}\text{Pb}$ versus $^{208}\text{Pb}/^{204}\text{Pb}$) showing the distribution of initial lead compositions of Greens Creek host rocks relative to model lead evolution curves and fields for modern petrotectonic environments.....	354
12. Initial strontium versus initial neodymium correlation diagram showing the distribution of initial Sr-Nd values for Greens Creek host rocks relative to model Sr-Nd fields for modern petro-tectonic environments	356
13. Initial lead versus initial neodymium correlation diagram showing the distribution of initial Pb-Nd values for Greens Creek host rocks relative to model lead-neodymium fields for modern petrotectonic environments	357
14. Initial strontium versus initial neodymium correlation diagram showing the distribution of initial Sr-Nd values for Greens Creek host rocks relative to Sr-Nd fields for previously published Alexander and Gravina terrane rocks	361
15. Pb-Pb correlation diagram ($^{206}\text{Pb}/^{204}\text{Pb}$ versus $^{207}\text{Pb}/^{204}\text{Pb}$) showing the distribution of initial lead compositions of Greens Creek host rocks relative to lead isotopic compositions for Greens Creek sulfides (ore).....	362

Radiogenic Isotopic Characterization and Petrogenesis of Host Rocks to the Greens Creek Deposit

Wayne R. Premo¹ and Cliff D. Taylor¹

Abstract

Samples representing the major host and adjacent lithologies at the Greens Creek deposit, Admiralty Island, were analyzed for their uranium-thorium-lead (U-Th-Pb), rubidium-strontium (Rb-Sr), and samarium-neodymium (Sm-Nd) isotopic systematics in order to provide petrogenetic information. A multisystematic procedure from a single-aliquot dissolution of whole-rock powders provided direct correlation of the isotopic systems in order to (1) characterize the tectonic environment(s) in which these rocks formed and provide a setting for the production of the Greens Creek style mineralization; (2) compare to other radiogenic isotopic results from various Upper Triassic rock suites throughout southeastern Alaska; and (3) compare with lead isotope data from Greens Creek ore (chap. 10) to determine the relationship of ore to host rock. The same set of isotopic data was evaluated for geochronologic purposes in chapter 11.

Initial Nd compositions at 215 Ma (average age for host rocks) of metabasalts and metagabbros varied between $\epsilon_{Nd} = +4$ to $+9$; whereas, initial $^{206}Pb/^{204}Pb$ and $^{87}Sr/^{86}Sr$ isotopic compositions at 215 Ma for the same suite of samples ranged from 18.45 to 18.92, and from 0.7037 to 0.7074, respectively, and are more enriched than mid-ocean ridge basalt values. These isotopic results are indicative of oceanic magmatic arcs environments and consistent with their derivation from a mostly depleted source(s) at about 215 Ma. Although initial Pb values from phyllite samples mimic those of the metabasaltic rocks, initial Sr and Nd values of phyllites are bimodal, some with $\epsilon_{Nd} = +8$, others with values at $+2$. Argillites have lower initial Nd (ϵ_{Nd} about -2 to $+2$), higher initial $^{206}Pb/^{204}Pb$ (18.4 to 19.0), and higher $^{87}Sr/^{86}Sr$ (0.705 to 0.707) than other host rocks, values that are typical for shales. These values suggest that the argillites contain some proportion of older, slightly more radiogenic crust. In general, initial Nd-Sr isotopic values for Greens Creek host rocks are comparable to previously published data from samples of the Alexander and Gravina terranes.

These radiogenic isotopic systematics indicate a progressively depleting source for the Upper Triassic Greens Creek rocks, suggesting a rift setting. The oldest argillites have slightly depleted signatures (ϵ_{Nd} about $+1.5$), that are unconformably overlain by a sequence of metabasalts that exhibit

depleted, island-arc-type isotopic signatures ($\epsilon_{Nd} = +4$ to $+5$ with elevated $^{87}Sr/^{86}Sr$ and $^{206}Pb/^{204}Pb$). The metabasalts are then unconformably overlain by conglomerate, dolomite, and more argillites of the Hyd Group. The Hyd Group argillites have slightly depleted to slightly enriched ϵ_{Nd} between -5 and $+2$, indicating the incorporation of some older, more enriched crustal material. The lower metabasaltic sequences are intruded by ultramafic sills and stocks, represented now as highly altered serpentinites that exhibit a wide range of isotopic signatures (ϵ_{Nd} between -12 and $+8$). Subsequent mafic volcanism and gabbroic plutonism are characterized by more depleted source signatures ($\epsilon_{Nd} = +5$ to $+9$). Hyd Group basalts that cap the Triassic section have even more depleted signatures ($\epsilon_{Nd} = +8$ to $+9$). This progressive sequence of least to most depletion implies opening of preexisting crust in a rift setting, probably within an oceanic arc environment.

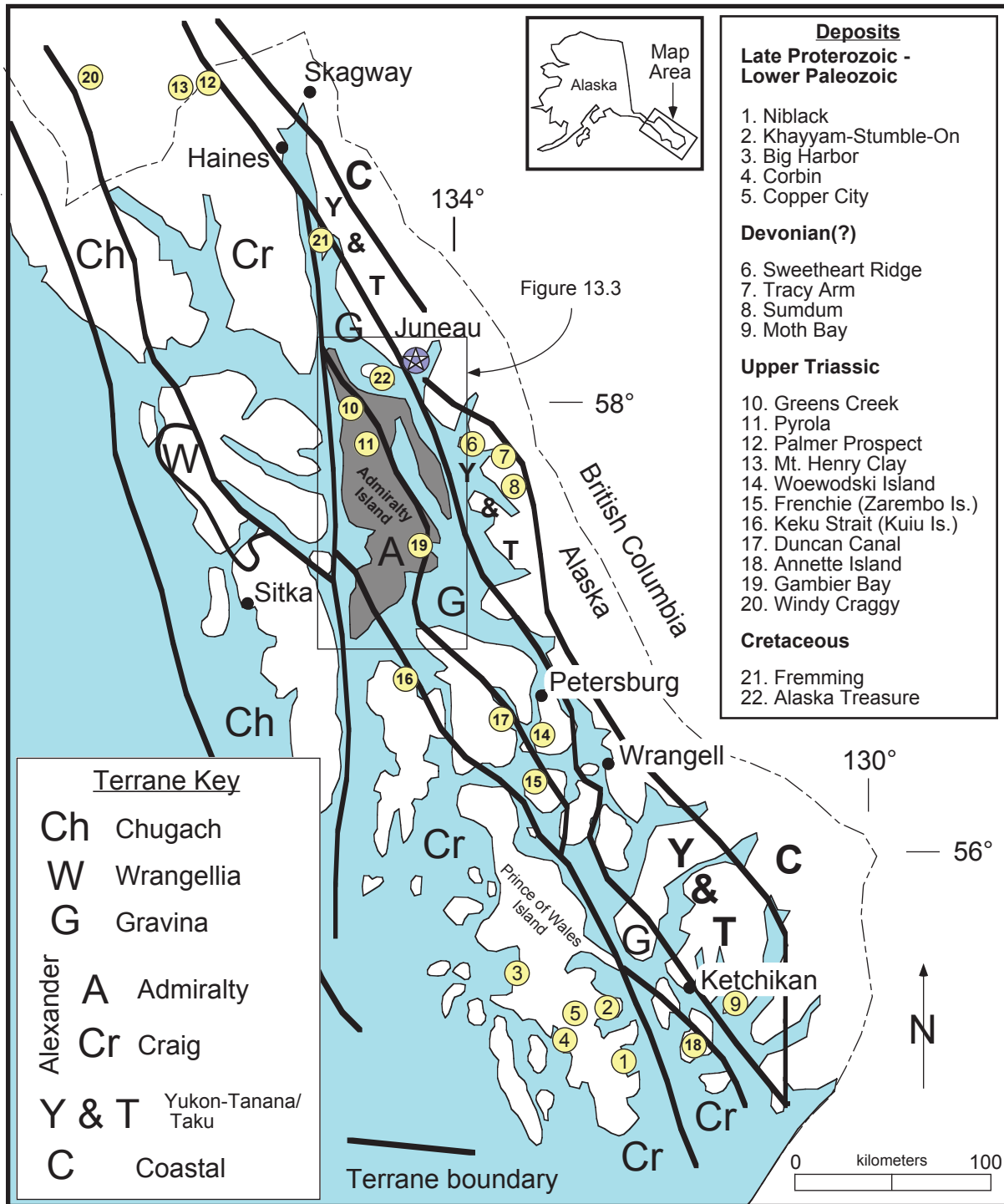
Initial Pb isotopic compositions of Greens Creek host rocks for the most part are not the same as Pb isotopic compositions for Greens Creek galena and other sulfides. However, it is evident that the relatively uniform ore Pb signature may represent a homogenization of Pb derived mainly from host basalt and gabbro, but also including some Pb from hanging-wall argillites, a Pb isotopic trend similar to those documented for volcanogenic massive sulfides (VMS) from modern rift zones and island-arc sequences.

Introduction

Volcanogenic massive sulfide (VMS) deposits are found in many locations and occurrences around the Pacific rim and particularly in Alaska. Their ages and styles vary somewhat, but most in Alaska are thought to originate in or near oceanic island-arc or rift-related settings (Newberry and others, 1997; Newberry and Brew, 1997). The ages for most of the VMS deposits of southeastern Alaska (fig. 1), and particularly within the Alexander terrane, are thought to be the same as their host rock sequences, such that the ore is syngenetic. In general, however, precise ages of mineralization are scarce. In approaching an age and origin for VMS deposits, particularly Greens Creek, radiogenic isotopic systems can be invaluable.

Radiogenic isotopic systems (U-Pb, Th-Pb, Sm-Nd, Rb-Sr, K-Ca, ^{40}Ar - ^{39}Ar , and Re-Os) can be and have been used

¹U.S. Geological Survey, Denver, Colorado.



for shedding light on the source(s) of mineralizing fluids (for example, Allegre and Luck, 1980; DePaolo, 1981; Zartman and Doe, 1981; Burke and others, 1982; Fehn and others, 1983; Zartman, 1984; Hart and Kinloch, 1989; Lambert and others, 1989; Walker and others, 1991; Kerrick, 1991; Martin, 1991; Ayuso and others, 2004). Previous radiogenic isotopic work on Greens Creek and other Late Triassic age VMS deposits of Alaska include lead (Pb) isotopic data of various sulfides, including galena, pyrite, and chalcopyrite (compiled in Gaccetta and Church, 1989, and references within; Newberry and Brew, 1997), and Rb-Sr and(or) Sm-Nd isotopic data from a variety of lithologic units from the Alexander, Stikine, Wrangellia, Gravina, and Taku terranes as well as samples from the Coast Mountains batholith (Samson and others, 1989, 1990, 1991a, 1991b).

An accurate yet simplistic interpretation of the Pb isotopic data for Alaskan VMS ore deposits including Greens Creek is discussed in Newberry and others (1997). These authors suggested that Pb isotopic compositions on sulfides from Alaskan VMS deposits are mixtures of mantle and crustal endmembers that exhibit apparent young model lead ages for ore deposition (fig. 2). Because crustal Pb compositions are typically more radiogenic (enriched ^{206}Pb) than mantle Pb compositions, the sulfide Pb isotopic compositions from various VMS deposits plot beyond the model-Pb evolution isochron at their actual ages. For example, Greens Creek and Pyrola ore Pb plots along the 0-Ma model lead isochron, although these deposits are constrained to have occurred in the Late Triassic (chap. 11). Other deposits exhibit Pb isotopic fields corresponding to futuristic model lead ages (for example, Mt. Henry Clay and Kuiu; figs. 1 and 2). This effect is thought to be the result of mixing between radiogenic crustal Pb and depleted mantle Pb in the source(s) prior to ore deposition. Mixing of these components might occur as continental crustal detritus is subducted beneath ore-producing oceanic island arcs. Whereas it is obvious that Pb isotopic data should not be used for model age determinations, they do hold promise in helping to identify possible source(s) for ore metals.

This explanation for radiogenic Pb signatures is testable using correlated Pb-Sr-Nd isotopic systematics from syngenetic, host-rock lithologies, isotopic signatures that should indicate to what degree crustal source(s) were involved in ore-forming processes as well as help delineate petroTECTONIC origins of various Phanerozoic allochthonous terranes of southeastern Alaska.

Greens Creek is located at the edge of the Alexander and Gravina Belt terranes (#10 in fig. 1), both of early Paleozoic to Jurassic-Cretaceous age. Positive initial ϵ_{Nd} (0 to +9) and low initial $^{87}\text{Sr}/^{86}\text{Sr}$ (0.7028 to 0.7071) isotopic values from volcanic, plutonic, and metasedimentary samples from these two terranes indicate that they were derived mainly from depleted mantle sources (Samson and others, 1989, 1991a) and were interpreted to represent Paleozoic island-arc terranes. Likewise, Sr-Nd isotopic data from samples of the adjacent Wrangellia terrane indicated a largely juvenile, mantle-derived

arc terrane with less than 6 percent Proterozoic crustal input (Samson and others, 1990).

In this chapter, we use several different radioactive decay schemes (U-Pb, Th-Pb, Rb-Sr, and Sm-Nd) to isotopically characterize in detail the host/source rocks of the Greens Creek ore deposit in order to better understand their petroTECTONIC derivation and provide a geologic framework and tectonic setting that produced sulfide deposition. Radiogenic isotopic signatures can further provide clues toward source(s) of ore-forming metals and fluids, helping to develop genetic ore deposit models and aid in the classification and prediction of known and potential deposits.

Geology

The geology at Greens Creek has been covered in detail in other chapters of this volume. Only a brief outline of the geology of the major host/source rocks that have been sampled is included here.

Greens Creek mine is 29 km south of Juneau, in the southeastern coastal region of Alaska, near the northern end of Admiralty Island (figs. 1 and 3). The deposit is located in an 800-km-long belt of volcano-sedimentary rocks interpreted to represent a rift-fill sequence formed during a brief period of intra-arc or back-arc rifting in latest Triassic time (Berg and others, 1972; Taylor, 1997; Taylor and others, 1995a, 1995b, 1999, 2000). Stratigraphy within the belt consists of a 200- to 800-m-thick sequence of conglomerates, limestones, marine clastic sediments, and tuffs that are intercalated with and overlain by a distinctive unit of mafic pyroclastics and pillowed flows (figs. 3 and 4). Faunal data bracket the age of the host rocks between early Carnian (early Late Triassic) and late Norian (late Late Triassic) time (fig. 4 and fig. 5, chap. 11).

At Greens Creek, the stratigraphy includes a Permian-age, siliceous to cherty argillite in the upper part of the Cannery Formation that is unconformably overlain by a sequence of metabasalts of unknown age (fig. 4). These metabasalts are variably metamorphosed at greenschist to amphibolite grade and subsequently altered during hydrothermal metasomatism (for example, Newberry and others, 1990), resulting in several types of phyllitic rocks. Geochemical signatures of many of these phyllites are not conclusive but are consistent with basaltic protoliths, either as a rift-related basalt produced in an intra-arc setting or as a fairly unfractionated calc-alkaline basalt formed in an oceanic volcanic arc. The arc-related signatures probably could be indicative of variable amounts of assimilation of preexisting island-arc crust.

These metabasalts are unconformably overlain by a thin, discontinuous polymictic conglomerate (fig. 4). Such conglomerates are found throughout the southern and middle portions of the Upper Triassic volcano-sedimentary belt at the base of most sections, indicative of high-energy deposition in a near slope or basin margin setting. Although thin and discontinuous conglomerate horizons occur in the northern half of Admiralty Island, their stratigraphic positions within

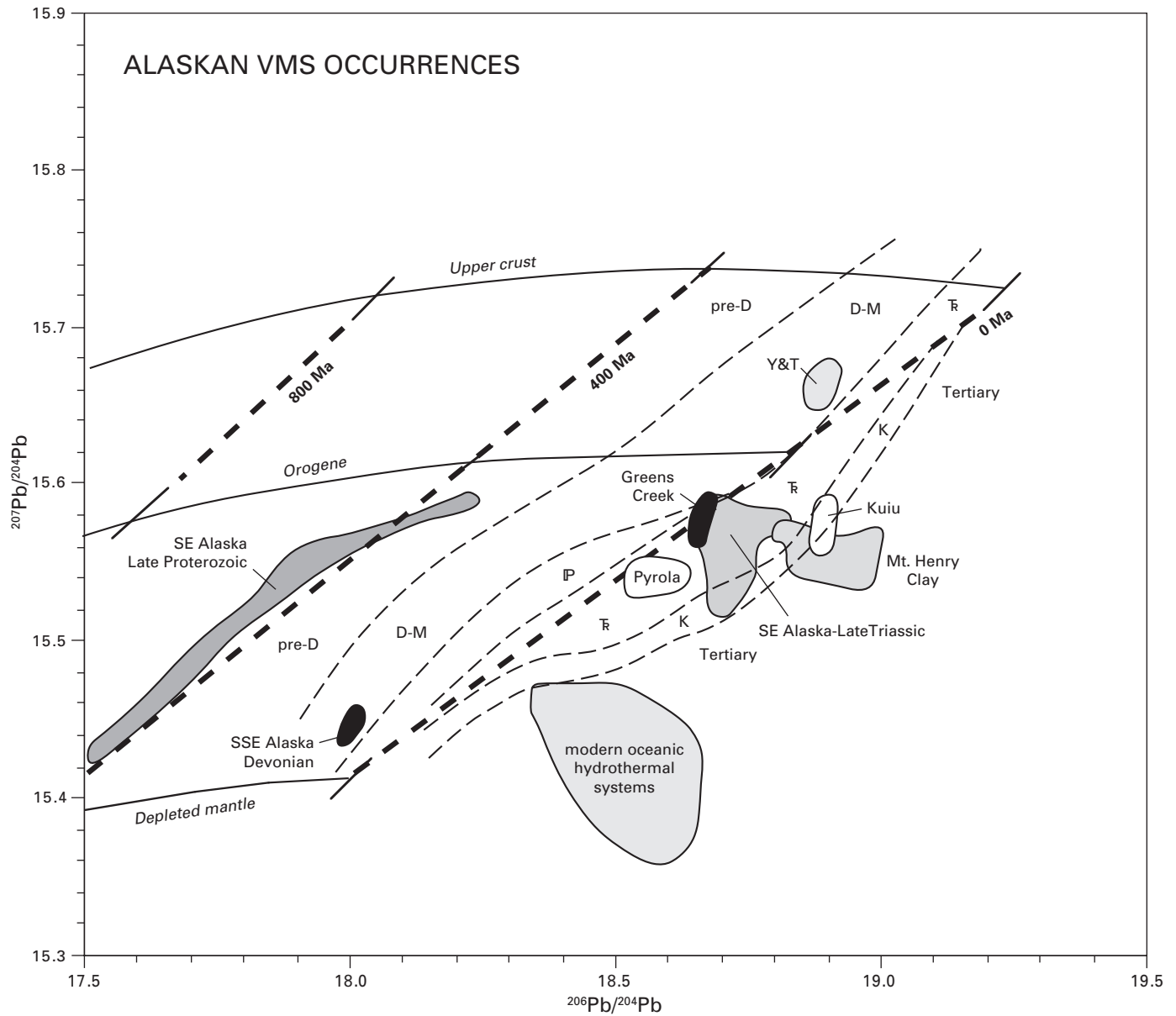
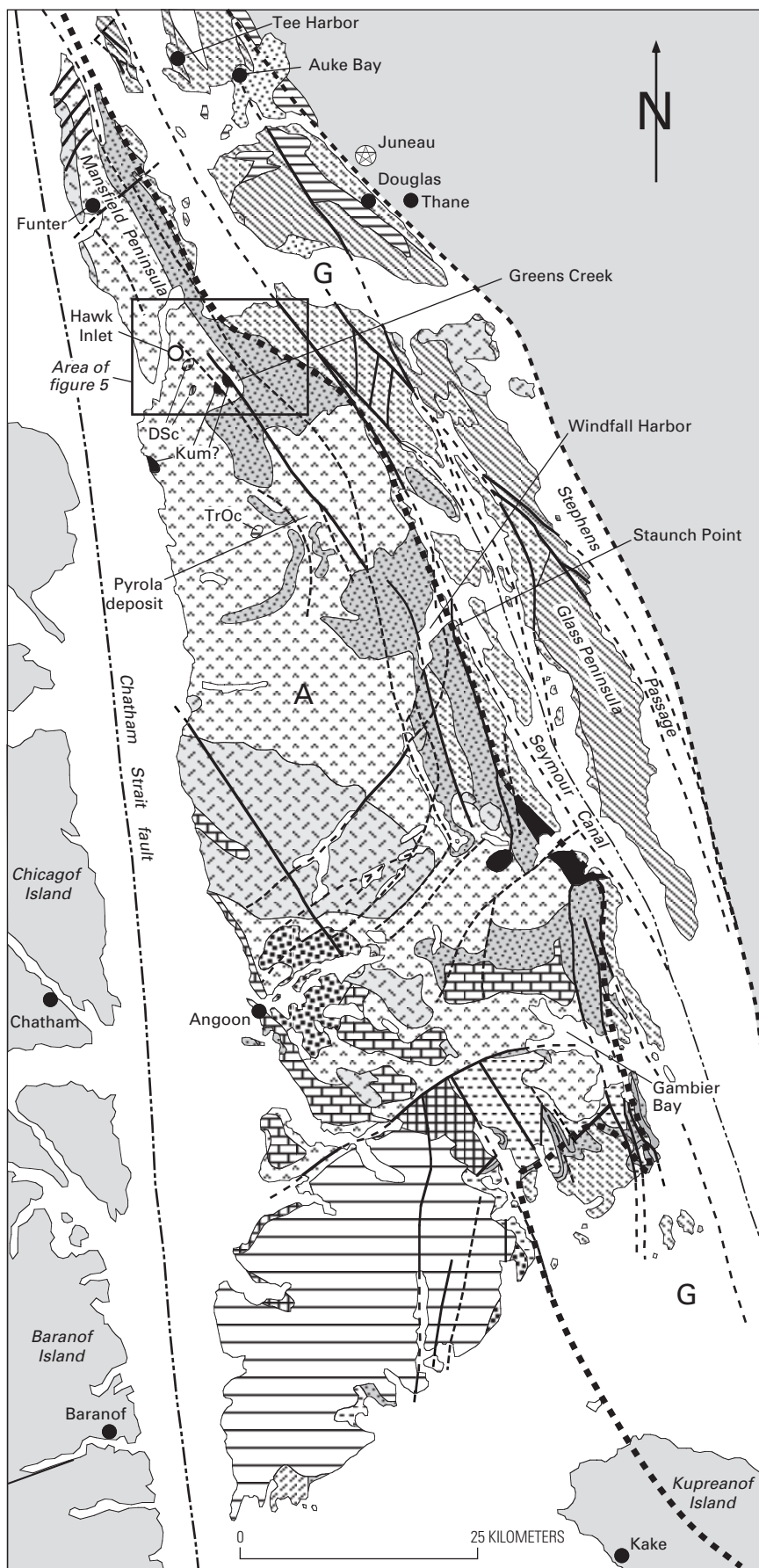


Figure 2. $^{206}\text{Pb}/^{204}\text{Pb} - ^{207}\text{Pb}/^{204}\text{Pb}$ correlation diagram showing the distribution of lead isotopic compositions (fields) for Alaskan volcanogenic massive sulfide (VMS) occurrences compared to model lead evolution curves ("upper crust," "orogene," and "depleted mantle") of Zartman and Doe (1981). Greens Creek ore compositions lie near other Late Triassic deposits such as Pyrola, Kuiu, and Mt. Henry Clay (modified from Newberry and others, 1997), at model lead ages (isochrons shown as bold dashed lines) younger than the actual age of mineralization (separated by lighter dashed lines and labeled; D = Devonian, D-M = Devonian to Mississippian, IP = Pennsylvanian, T = Triassic, K = Cretaceous). Y & T indicates the location of lead isotopic results from ores of the Yukon-Tanana/Taku terrane.



EXPLANATION

- Quaternary surficial sediments
- Tertiary volcanic rocks
- Tertiary sedimentary rocks
- Cretaceous granitoids
- Cretaceous ultramafic rocks
- Cretaceous-Jurassic sedimentary rocks
- Cretaceous-Jurassic volcanic and sedimentary rocks
- Cretaceous-Jurassic volcanic rocks
- Triassic-Permian sedimentary and volcanic rocks, undifferentiated
- Triassic-Ordovician sedimentary and volcanic rocks, undifferentiated
- Triassic-Ordovician carbonate rocks, undifferentiated.
- Permian sedimentary rocks
- Permian carbonate rocks
- Devonian-Silurian carbonate rocks
- Silurian sedimentary rocks
- Silurian-Ordovician sedimentary rocks
- Other rocks
- Major fault
- Inferred fault trace
- Terrane boundary

Figure 3. Simplified geologic map of Admiralty Island, showing locations for Greens Creek and Pyrola deposits, Gambier Bay, Windfall Harbor, the Mansfield Peninsula, and Staunch Point (locations of some whole-rock samples). Bold dotted line is approximate boundary between the Alexander (A) and Gravina (G) terranes (after mapping by Gehrels and Berg, 1992).

the Triassic stratigraphy are uncertain and in most cases are thought to be above the base of the section within the shales that compose the middle sedimentary portion of the Triassic stratigraphy. The northernmost occurrence of a conglomerate “marker horizon” at the base of the section is on the eastern shore of Windfall Harbor (fig. 3) immediately overlying the siliceous black shales of the Cannery Formation.

Thin carbonate beds lie just below and intercalated with the capping Hyd Group basalts and are intercalated with the shales (argillites). North of Admiralty Island, limestones appear to be absent from the section.

Serpentinities are clearly produced by alteration of an ultramafic protolith and probably represent the shallow intrusive sources to the primitive basalt protoliths or to the overlying Hyd Group mafic volcanic flows. Many of these serpentinite bodies were probably cumulates left after extraction of mafic melts. These serpentinites crosscut the older metabasalt and phyllite sequences as well as the basal conglomerate horizon (figs. 3 and 4). Gabbro-clinopyroxenite, both relatively fresh and highly quartz-carbonate-fuchsite-altered serpentinite, is a common outcrop occurrence in the mine area. It is likely that the footwall phyllite pile originally consisted of a composite mafic-ultramafic collection of massive to volcanoclastic textured volcanics.

These mafic/ultramafic rocks are in turn overlain by massive and slaty graphitic, pyritic, black argillites and by carbonate-rich dolomitic massive and slaty argillites of the Hyd Group.

Continued emplacement of basaltic magmas at shallow levels account for the common occurrence of large gabbroic sills and stocks, particularly exposed along Gallagher Ridge, south of the mine (fig. 5), and followed by mafic flows of the overlying Hyd Group (fig. 4). Continued production of heat in the immediate footwall of the deposit would similarly account for the extreme alteration of the gabbro-basalt pile by driving a hydrothermal convection system.

Diabase dikes are observed to crosscut massive ore and are, at this point, not well understood. It is likely that these dikes are the product of Jurassic-Cretaceous resumption of island-arc volcanism. The fact that they crosscut ore and the overlying argillites and themselves are mineralized with a late, precious-metal-enriched mineral assemblage brackets their age between 220 Ma and the 105- to 90-Ma mid-greenschist facies regional metamorphism.

The Greens Creek massive sulfides are located at the contact between a footwall sequence of predominantly mafic volcanic rocks and mafic-ultramafic hypabyssal sills and intrusions, and a hanging wall of black argillites (figs. 4 and 6A). With increasing proximity to ore, footwall lithologies are dominated by chlorite-phyllites, sericite-phyllites, and silicified sericite-phyllites (fig. 6B). Footwall lithologies which have less consistent spatial distribution are serpentine-chlorite phyllites, mariposite-phyllites, and rarely, recognizable gabbros and post-ore diabase dikes. Hanging-wall rocks are dominated by massive and slaty graphitic, pyritic, black argillites and by carbonate-rich dolomitic massive and slaty argillites. Three

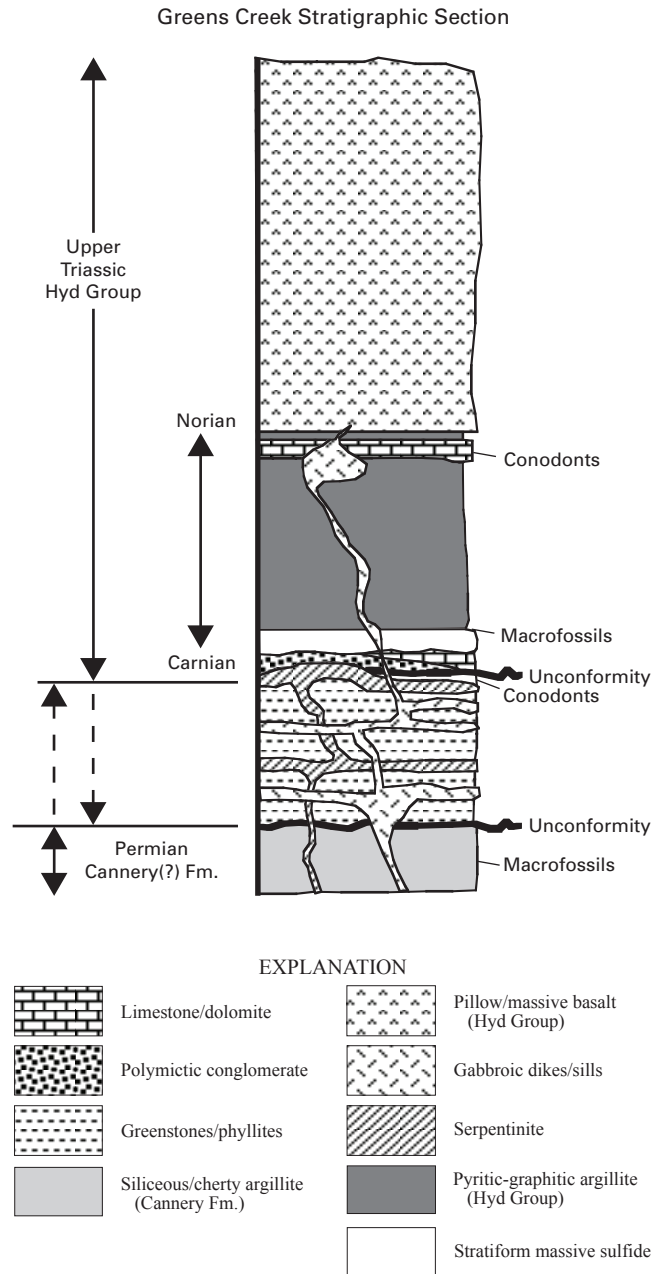
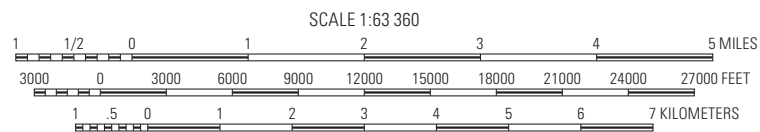


Figure 4. Stratigraphy of the Greens Creek section, Admiralty Island, showing the orebody at the contact between footwall phyllites and hanging-wall argillites (after Taylor and others, 2000).



Figure 5. Map of surface sampling sites at and near Greens Creek mine, Admiralty Island. Single-numbered locations are from the 97-LG series (for example, "82" is the location of 97-LG-82, and so forth). PF-series (-09 and -18) are from the Portal Face. Topographic map compiled from USGS Juneau A3 and A2 1:63,360 scale, 1997.



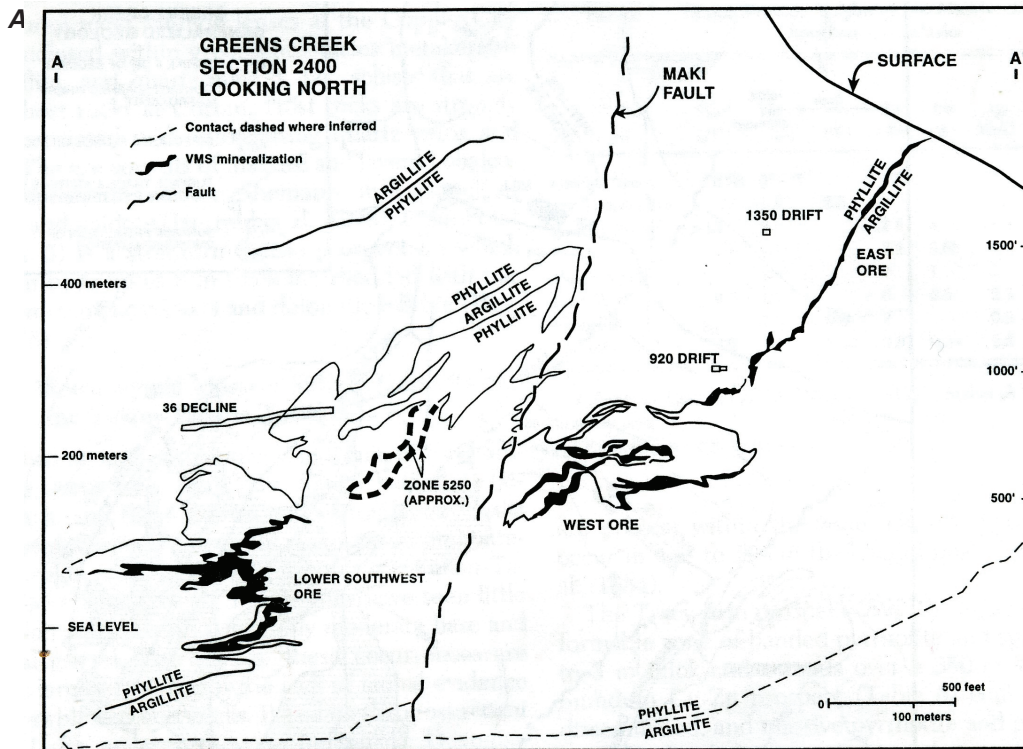


Figure 6. (A) Geologic cross section, Greens Creek mine. Courtesy of T. Hall, senior mine geologist, Kennecott Greens Creek Mining Co., 1995. VMS = volcanogenic massive sulfide (after Newberry and others, 1997), showing the orebody at the contact between footwall phyllites and hanging-wall argillites. Locations are shown for East, West, and the Southwest orebodies where samples of sulfides, host rocks, and alteration minerals for Ar–Ar work were collected.

major contiguous orebodies lie along a single horizon marked by a footwall greenschist and a hanging wall composed of graphitic, pyritic, black argillite. Ores are zoned from silica-, carbonate-, and barite-rich white ores against the footwall, to massive pyritic, and then to base-metal-rich massive sulfide-rich ores against the hanging wall (fig. 6).

Sampling

Ore deposits form from mineralizing fluids that have passed through a sequence of rocks and therefore have had some contact with various lithologies of differing geochemical signatures and isotopic compositions. The result is very likely a mixture of several components. Geochemical and isotopic data for the host/source rocks are therefore critical toward a clear interpretation of the isotopic signature of the ore. In addition, identification of multiple fluids and ore-forming stages can be crucial to evaluating the isotopic information.

Certain geologic conditions can unequally disrupt the stability and therefore the reliability of isotopic results. For example, elemental mobility through alteration and/or metamorphism, can fractionate parent-daughter ratios and disturb the isotopic systematics. In general, a hierarchy of stability during

metamorphism is recognized: Sm–Nd > U–Pb > Rb–Sr; however, extreme alteration can greatly affect any of the systematics.

Consequently, radiogenic isotopic systematics of altered rocks are often disturbed, yielding results that are not easily interpretable — interpretations that are necessary for distinguishing between syndepositional, tectonic, magmatic, or hydrothermal processes. Therefore, careful sampling of both ore and host/source rock is a critical aspect for the successful use of radiogenic isotopic systems on ore deposits.

With these possible difficulties in mind, only the best preserved and most representative samples (listed in table 3, chap. 11) were carefully selected from several hundred other samples for this multisystematic isotopic analysis. U–Th–Pb, Rb–Sr, and Sm–Nd isotopic data from whole-rock powders and mineral separates were collected from Greens Creek host rocks and related units that include (1) a variety of argillites, both from the Cannery Formation and the Hyd Group, collected from inside and outside the mine; (2) various metabasalts including some from the Gambier Bay Formation and the Hyd Group; (3) various metagabbroic to ultramafic intrusives (serpentinites) of Late Triassic age, some perhaps slightly older or younger; (4) associated chloritic to sericitic phyllites that probably represent altered mafic volcanic rocks (Newberry and others, 1990), collected from inside and outside the mine proper; and (5) several crosscutting diabasic to dioritic intrusives of unknown age.

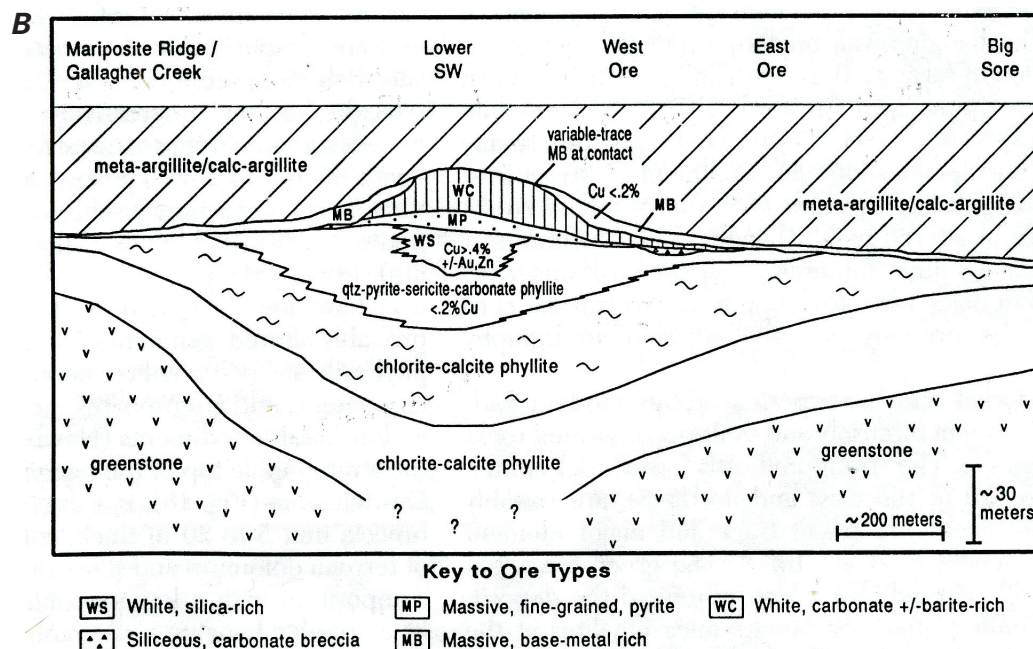


Figure 6. (B) Predeformation, cross-sectional model, Greens Creek deposit, based on drill-core logging and underground and surface mapping (Rainer Newberry, unpub. mapping, 1985–1994; after Newberry and others, 1997), again showing the orebody (mainly MB and MP) at the contact between footwall phyllites and hanging-wall argillites, but also the distribution and relationship of several types of footwall phyllites within the alteration zone of the mine area (see table 3 in chapter 11 for whole-rock sample designations).

Surface sampling sites around the Greens Creek mine are shown in figure 5; mine sample locations are more problematic and are simply stated in table 3 in chapter 11. Locations of samples from other parts of Admiralty Island are not shown but generally given in table 3, chapter 11, by their geographic location (for example, Gambier Bay, Pyrola, Staunch Point). Also, for the full names of samples used for whole-rock isotopic work, the reader is directed to tables 3 through 6, chapter 11, as many of the sample names have been shortened in this text and in the figures by removing the front numbers corresponding to their year of collection (for example, LG-71 in the text is actually 97–LG-71 in the tables).

Results

The data were produced in order to calculate initial Pb-Sr-Nd isotopic compositions that can be compared with known, time-integrated, isotopic fields from different petrotectonic environments. This exercise is intended to delineate the geologic framework and tectonic setting in which Greens Creek and possibly other VMS deposits of southeastern Alaska were formed as well as to contribute to the growing isotopic database for such rocks for use in the scientific community at large. The U-Pb, Rb-Sr, and Sm-Nd isotopic data are

given in tables 4 through 6 in chapter 11, where the same data were evaluated for geochronologic purposes.

The analytical techniques used for the simultaneous, single-dissolution of U-Th-Pb, Rb-Sr, and Sm-Nd analysis on whole-rock and mineral separates were similar to those reported by Tatsumoto and Unruh (1976) and Premo and Tatsumoto (1991, 1992) and are given in detail in chapter 11.

Degree of Stability of the Isotopic Systematics

There is some concern as to whether the isotopic systematics of these whole rocks, which have certainly been altered to some degree (table 3 in chap. 11), have remained stable or undisturbed. The processes of alteration involve mobilization of certain elements, and it is probable that elemental concentrations as well as their corresponding Pb-Sr-Nd isotopic compositions are to some degree disturbed in some samples. However, we expect that the Sm-Nd systematics are less affected than the more mobile and volatile Rb-Sr and U-Pb systematics (for example, Whitehouse, 1988; Barovich and Patchett, 1992).

There is no way to absolutely ascertain to what degree any particular isotopic system is undisturbed or overprinted without fresh, unaltered samples to compare. However, we expect that varying degrees of alteration should reflect the

relative stability of their isotopic systematics. For example, the least-altered samples are the Hyd Group metabasalts from Gambier Bay (fig. 3) and their isotopic systematics are arguably the best preserved and are used to construct several isochron ages (chap. 11). In contrast, the isotopic systematics of highly altered serpentinites vary widely, and little confidence can be held for these results.

In an attempt to evaluate the degree of isotopic disturbance, uranium concentration in parts per million (ppm) is plotted against calculated initial $^{206}\text{Pb}/^{204}\text{Pb}$ values at 215 Ma (taken to be an average estimate of the age of the host-rock strata at Greens Creek; chap. 11) and Rb (ppm) against calculated initial $^{87}\text{Sr}/^{86}\text{Sr}$ values (fig. 7). Because we have defined an isochron age of 218 ± 16 Ma and initial $^{206}\text{Pb}/^{204}\text{Pb}$ value of 18.515 for the Hyd Group metabasalts (chap. 11), this value is taken to represent the Greens Creek host-rock initial lead signature to which all other initial values can be compared (fig. 7A). In addition, the majority of sulfide lead (mainly galena) from the Greens Creek deposit defines a $^{206}\text{Pb}/^{204}\text{Pb}$ isotopic composition of 18.64 ± 0.01 that we interpret to represent that of the mineralizing fluid that probably altered many of the host rocks. Therefore, samples that yielded initial $^{206}\text{Pb}/^{204}\text{Pb}$ values outside of the 18.515 to 18.640 range are suspected of either having some subsequent open-system isotopic disturbance or derivation from a distinctly different isotopic source. In some cases, the calculated initial $^{206}\text{Pb}/^{204}\text{Pb}$ values are unreasonably low such that the addition of uranium or loss of lead during subsequent alteration is suspected (for example, LG-71 and ADM-01; fig. 7A). In some other cases where the calculated initial $^{206}\text{Pb}/^{204}\text{Pb}$ values are significantly higher than 18.64, the addition of lead with a more radiogenic composition is suspected. This situation is reasonable as nearby Cretaceous-Tertiary ore $^{206}\text{Pb}/^{204}\text{Pb}$ signatures are between 19.1 and 19.5 (discussed herein and also in chapter 10) and certainly could have been involved in a partial resetting of the lead isotopic composition of some lithologies (for example, some Hyd Group argillites and sample GST; fig. 7A).

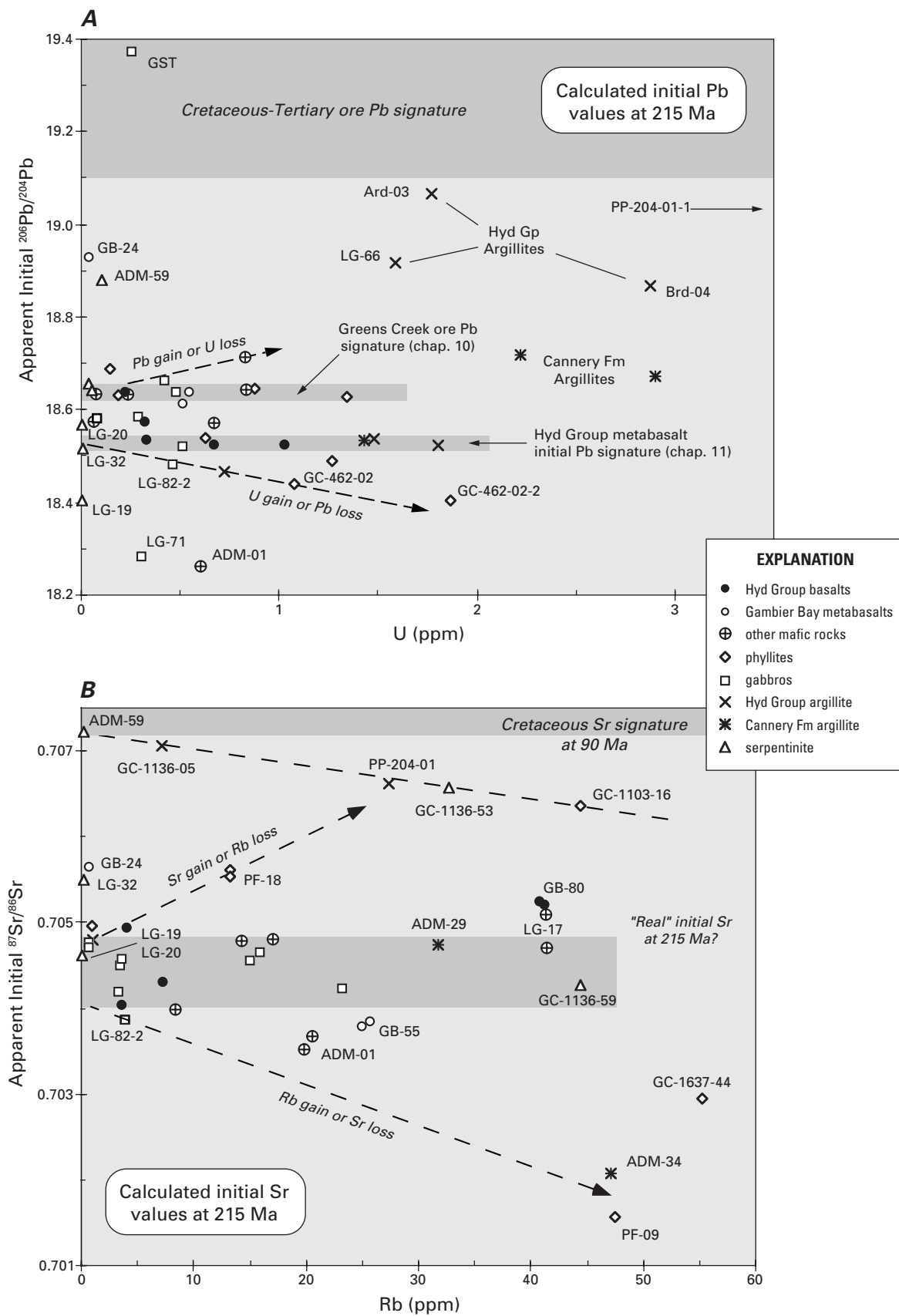
A similar situation can be made in the case of rubidium concentration (ppm) versus calculated initial $^{87}\text{Sr}/^{86}\text{Sr}$ values (fig. 7B). The majority of least-altered mafic samples (for example, Hyd Group metabasalts and metagabbros at Gallagher Ridge) define a range of initial $^{87}\text{Sr}/^{86}\text{Sr}$ values between 0.7038 to 0.7048 that we tentatively regard as the range of the original Greens Creek host-rock initial strontium composition. And all other samples that yielded initial strontium values outside that range, we suspect either have had some subsequent open-system isotopic disturbance or derivation from a distinctly different isotopic source. For example, samples PF-09 and ADM-34 yielded unreasonably low calculated initial $^{87}\text{Sr}/^{86}\text{Sr}$ values (less than 0.7023) and are therefore suspected of having secondary rubidium added during alteration (fig. 7B). This suspicion is reasonable as sericitization would involve alteration to micaceous minerals with the addition of potassium (K) and Rb. Other samples with “low” calculated initial $^{87}\text{Sr}/^{86}\text{Sr}$ values (less than 0.7038) may have had secondary rubidium added to lesser degrees. In cases where the calculated initial $^{87}\text{Sr}/^{86}\text{Sr}$

Figure 7 (facing page). (A) Plot of uranium (U) concentration versus calculated initial $^{206}\text{Pb}/^{204}\text{Pb}$ at 215 Ma for whole-rock analyses of major Greens Creek host rocks, illustrating the possible isotopic disturbance of some whole-rock samples, probably during alteration. The expected range of initial $^{206}\text{Pb}/^{204}\text{Pb}$ values is between 18.515 (Hyd Group metabasalt initial lead (Pb) and 18.64 (Greens Creek ore lead signature). All samples outside of this range are either isotopically disturbed or derived from distinctly different source(s). (B) Plot of rubidium (Rb) concentration versus calculated initial $^{87}\text{Sr}/^{86}\text{Sr}$ at 215 Ma for whole-rock analyses of major Greens Creek host rocks. Similar to the lead results, these strontium results possibly indicate isotopic disturbance within some whole-rock samples. The expected range of initial $^{87}\text{Sr}/^{86}\text{Sr}$ values is indicated by the least altered or best preserved Hyd Group metabasalts that indicate values between 0.7041 and 0.7049, and all samples with initial $^{87}\text{Sr}/^{86}\text{Sr}$ values outside this range are either isotopically disturbed or derived from distinctly different source(s). Ma, mega-annum. See text for further discussion.

values are significantly higher than about 0.7048, the addition of secondary radiogenic strontium is suspected. A likely source for this secondary radiogenic strontium would be seawater alteration at just about any time after formation as all seawater strontium isotopic compositions from the Triassic to the present have been more radiogenic than 0.7065 (Burke and others, 1982; Hess and others, 1986).

In another evaluation of possible alteration or contamination of some of these samples by subsequent elemental and isotopic exchange, calculated initial $^{206}\text{Pb}/^{204}\text{Pb}$ and $^{87}\text{Sr}/^{86}\text{Sr}$ values are plotted against calculated initial ϵ_{Nd} values at 90 Ma (fig. 8). This age corresponds to average ages defined by isochrons from the same isotopic data and similar to Ar-Ar isotopic data from sericite and fuchsite (chap. 11), and the age therefore represents a very likely time that some of the isotopic systems were disturbed. In figure 8A, nearly 6 of 10 argillitic and 3 of 8 metagabbroic samples yielded initial $^{206}\text{Pb}/^{204}\text{Pb}$ values at 90 Ma between 19.1 and 19.55, values that are very similar to lead isotopic compositions of Cretaceous to early Tertiary age, southeastern Alaskan ore deposits (for example, Alaska-Juneau, Ascension, Ground Hog, Perseverance, Trokna Silver, and Glacier Basin; Gaccetta and Church, 1989). These values are also very similar to those measured on the Cretaceous-Tertiary, arc-related, Valdez and Orca Group argillites and phyllites of southern Alaska (Farmer and others, 1993).

The suggestion here is that a Cretaceous-Tertiary lead signature may have overprinted several samples of argillite (ADM-29, Ard-03, PP-204-01, and Brd-04) and/or gabbro (GST, LG-69, LG-82) during the already established Cretaceous accretionary event at ca. 115 to 90 Ma (for example, Rubin and



others, 1990; Rubin and Saleeby, 1992), although alteration at any time after emplacement of these rock sequences may contribute to a disturbance of the U-Pb isotopic systematics. All of these samples yielded calculated $^{206}\text{Pb}/^{204}\text{Pb}$ values at 215 Ma outside the expected range of values (fig. 7A).

Another point of interest, six of nine phyllites and several other mafic samples exhibit calculated $^{206}\text{Pb}/^{204}\text{Pb}$ values at 90 Ma that are similar to the Greens Creek ore lead signature (fig. 8A), suggesting that the lead isotopic compositions of these samples had been overprinted during the Cretaceous. However, many of the better-preserved samples (for example, Hyd Group metabasalts and some metagabbros) yielded expected initial $^{206}\text{Pb}/^{204}\text{Pb}$ values at 215 Ma and keep a tight cluster through time (fig. 8), lending confidence to these whole-rock isotopic data.

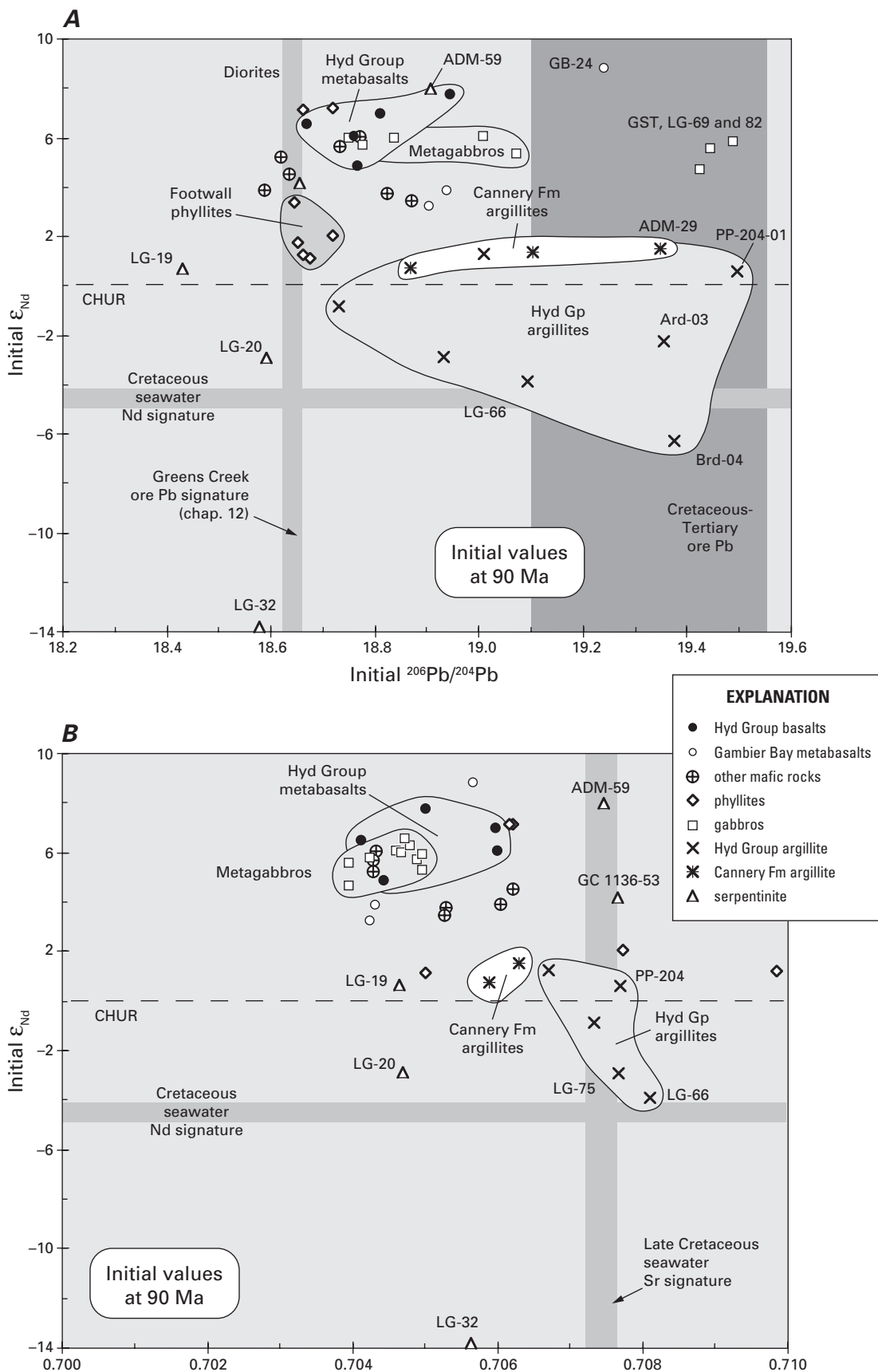
Similar to initial $^{206}\text{Pb}/^{204}\text{Pb}$ values suggestive of Cretaceous resetting, initial $^{87}\text{Sr}/^{86}\text{Sr}$ isotopic compositions for several argillites, phyllites, and serpentinites at 90 Ma (fig. 8B) are similar to the range of Late Cretaceous seawater strontium isotopic compositions (about 0.7074; Burke and others, 1982; Hess and others, 1986). Metagabbros, metabasalts, and other mafic samples appear relatively stable with initial $^{87}\text{Sr}/^{86}\text{Sr}$ values between 0.703 and 0.706, but initial strontium values for serpentinites, phyllites, and argillites vary widely, some remaining similar to those of the igneous suite, and others enriched with values near or at the Cretaceous-Tertiary seawater signature at about 90 Ma (fig. 8B). It may be coincidence that several are similar to this seawater value, but the variation would suggest some disturbance to the strontium isotopic systematics, perhaps due to Rb/Sr fractionations during alteration.

Sm-Nd isotopic systematics can be compared between lithologies and their differences evaluated — caused largely due to source differences and not because of alteration or age effects. Stability of the Sm-Nd isotopic system for some of the better-preserved samples appears to be good (fig. 9, chap. 11), and due to a fortunate spread in parent-daughter ratios, isochrons can be fitted to some of the analyses of two suites of samples. Four out of five Hyd Group metabasalt analyses define an apparent isochron age of 215 ± 95 Ma and four analyses from metagabbro samples LG-70 and LG-71 yielded an isochron age of 200 ± 27 Ma (chap. 11). Metagabbros and metabasalts have elevated $^{143}\text{Nd}/^{144}\text{Nd}$ (corresponding to initial ϵ_{Nd} values of +5.5 to 8) compared to coeval argillitic metasediments and most phyllites (less than 0.5128; initial ϵ_{Nd} = -2.5 to +4). Cannery Formation argillites yield uniform $^{143}\text{Nd}/^{144}\text{Nd}$ values at about 0.51266 (initial ϵ_{Nd} about +2.3) that contrast with Hyd Group argillites signatures (initial ϵ_{Nd} about -5 to +2.2). Serpentinites vary from very low $^{143}\text{Nd}/^{144}\text{Nd}$ (ϵ_{Nd} = -12.5; LG-32) to very high $^{143}\text{Nd}/^{144}\text{Nd}$ (ϵ_{Nd} = +8.4; ADM-59), indicating highly variable crustal to mantle source(s) for the ultramafic equivalents (fig. 9). However, because of very low Sm-Nd abundances in these samples, most of these isotopic analyses were obtained during low ion-beam intensity measurements that could produce results of questionable quality (see table 6, chap. 11). Therefore, the Sm-Nd isotopic differences in the serpentinites are regarded with skepticism and

Figure 8 (facing page). (A) A comparison of calculated initial $^{206}\text{Pb}/^{204}\text{Pb}$ versus initial ϵ_{Nd} for whole rocks analyses from Greens Creek host rocks at 90 Ma. Because the Greens Creek section is known to have undergone at least greenschist metamorphism during the Cretaceous (ca. 115 to 90 Ma; Rubin and others, 1990; Rubin and Saleeby, 1992), initial Pb-Nd values were calculated back to 90 Ma for a comparison with known Late Cretaceous-Tertiary ore lead compositions (for example, Gaccetta and Church, 1989) and contemporaneous arc-related sediments (Farmer and others, 1993). Some whole-rock samples, particularly argillites and three metagabbros, have similar lead isotopic composition to Cretaceous-Tertiary ore deposits at 90 Ma, suggesting the possibility that these samples were overprinted by this lead isotopic composition. It could also be coincidence, although all other whole-rock samples do not plot near this composition at 90 Ma with the possible exception of metabasalt, GB-24. Pb, lead; Nd, neodymium; Ma, mega-annum; CHUR, chondritic uniform reservoir. (B) A comparison of initial $^{87}\text{Sr}/^{86}\text{Sr}$ versus initial ϵ_{Nd} for whole rocks analyses from Greens Creek host rocks at 90 Ma. Again, because the Greens Creek section is known to have undergone at least greenschist metamorphism during the Cretaceous (ca. 115 to 90 Ma; Rubin and others, 1990; Rubin and Saleeby, 1992), initial Sr-Nd values were calculated back to 90 Ma for a comparison with known Late Cretaceous-Tertiary seawater strontium compositions (for example, Burke and others, 1982; Hess and others, 1986). Again, some argillites (but not the same argillites), two phyllites, and two serpentinites appear to have possibly been affected or overprinted by Cretaceous-Tertiary seawater strontium. This observation may only be coincidence. However, in general, only relatively high Rb/Sr rocks show any appreciable variation between 215 and 90 Ma, and these rocks are mostly argillites and phyllites that contain a greater proportion of micaceous minerals. Sr, strontium; Nd, neodymium; Ma, mega-annum; CHUR, chondritic uniform reservoir.

are included here for the sake of completeness and discussion in the event they may be accurate, though imprecise.

Because the Sm-Nd systematics were obtained from whole rocks, some associations can be made: (1) metabasalts GB-22, GB-42, and GB-80, and phyllite PF-18; (2) ADM-01, AD-58, perhaps GB-59, and most of the metagabbros; (3) metabasalts GB-55, ADM-12, perhaps LG-17, phyllite GC-1637-44, and the serpentinite GC-1136-53; (4) phyllites GC-462-02, GC 462-07, and PF-09 with argillites PP-204-01, LG-78, ADM-29, ADM-34, NAD T4-2, and serpentinite LG-19; and (5) argillites Ard-03, LG-75, and serpentinite LG-20. As will be discussed later, these Sm-Nd isotopic differences are largely indicative of source material such that low $^{143}\text{Nd}/^{144}\text{Nd}$ compositions (and correspondingly low or negative ϵ_{Nd} values) indicate contamination from an older, more enriched, crustal source, and that the progression of negative to positive ϵ_{Nd} values may well indicate the evolution of a rifting event within the Alexander terrane.



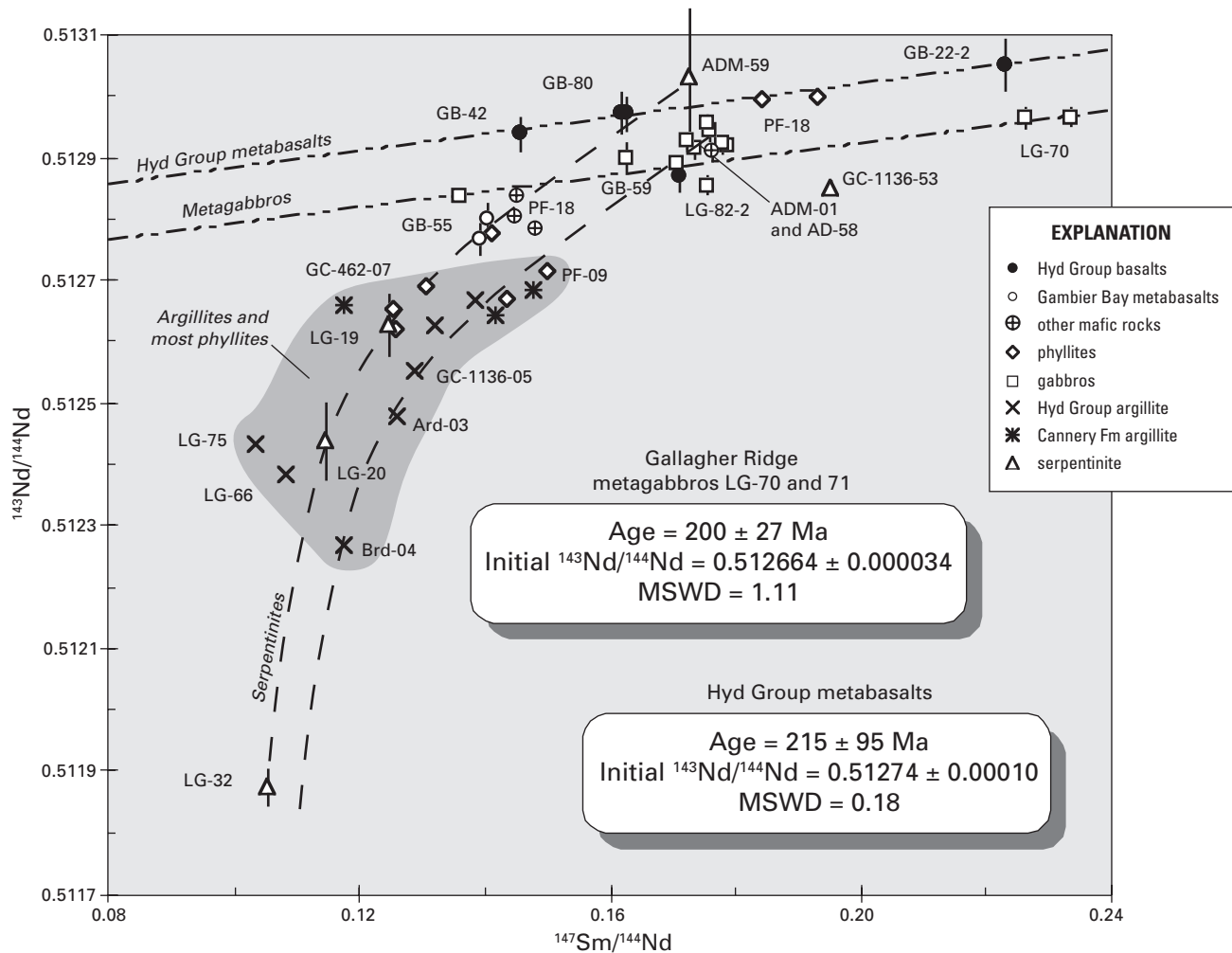


Figure 9. A comparison of the samarium-neodymium isotopic systematics of Greens Creek host rocks to Hyd Group metabasalt and Gallagher Ridge metagabbro isochrons, showing the extent of isotopic stability or variation within the different lithologic units. Argillites and phyllites are significantly more enriched than the metabasalt and metagabbro suites, indicating older crustal input or subsequent alteration. Serpentinities are conspicuously different, initial ϵ_{Nd} ranging from +8 (ADM-29) to -12 (LG-32), indicating distinctly different sources, probably at significantly different ages. MSWD, mean square of weighted deviates.

Initial Lead, Strontium, and Neodymium Isotopic Systematics of Greens Creek Host-Rock Lithologies

In figures 10 and 11, initial lead isotopic values (calculated at 215 Ma, Hyd Group metabasalt age) for Greens Creek host rocks are compared to model lead compositions from several major, planet-scale, lead reservoirs (Zartman and Doe, 1981). The lead isotopic evolution of these lead reservoirs is illustrated by separate curves emanating from a much older reservoir (ca. 4,000 Ma) that underwent planet-scale U/Pb fractionations. Average isotopic compositions of these separate lead reservoirs over the Phanerozoic are labeled “depleted mantle,” “orogene,” “lower crust,” and “upper crust.” Readers should bear in mind that these curves

represent the path of average values and do not convey the ranges of values that are possible for these reservoirs. Also, the “upper crust” curve is defined from mostly Phanerozoic data, such that lead from much older (for example, Archean to Proterozoic) crustal sources could be considerably more radiogenic with much higher $^{207}\text{Pb}/^{204}\text{Pb}$ values at equal $^{206}\text{Pb}/^{204}\text{Pb}$ compositions. Readers are referred to Dickin (1995) for a more detailed discussion of the U-Pb evolution of the Earth and its major reservoirs.

Important advantages can be found in the correlation of the two U-Pb decay schemes; one, they are geochemically similar, eliminating any effects due to natural fractionation processes; and two, their decay constants are different enough to cause a pronounced nonlinear correlation between them, and greater separation and distinction of their lead evolution curves (fig. 10). The

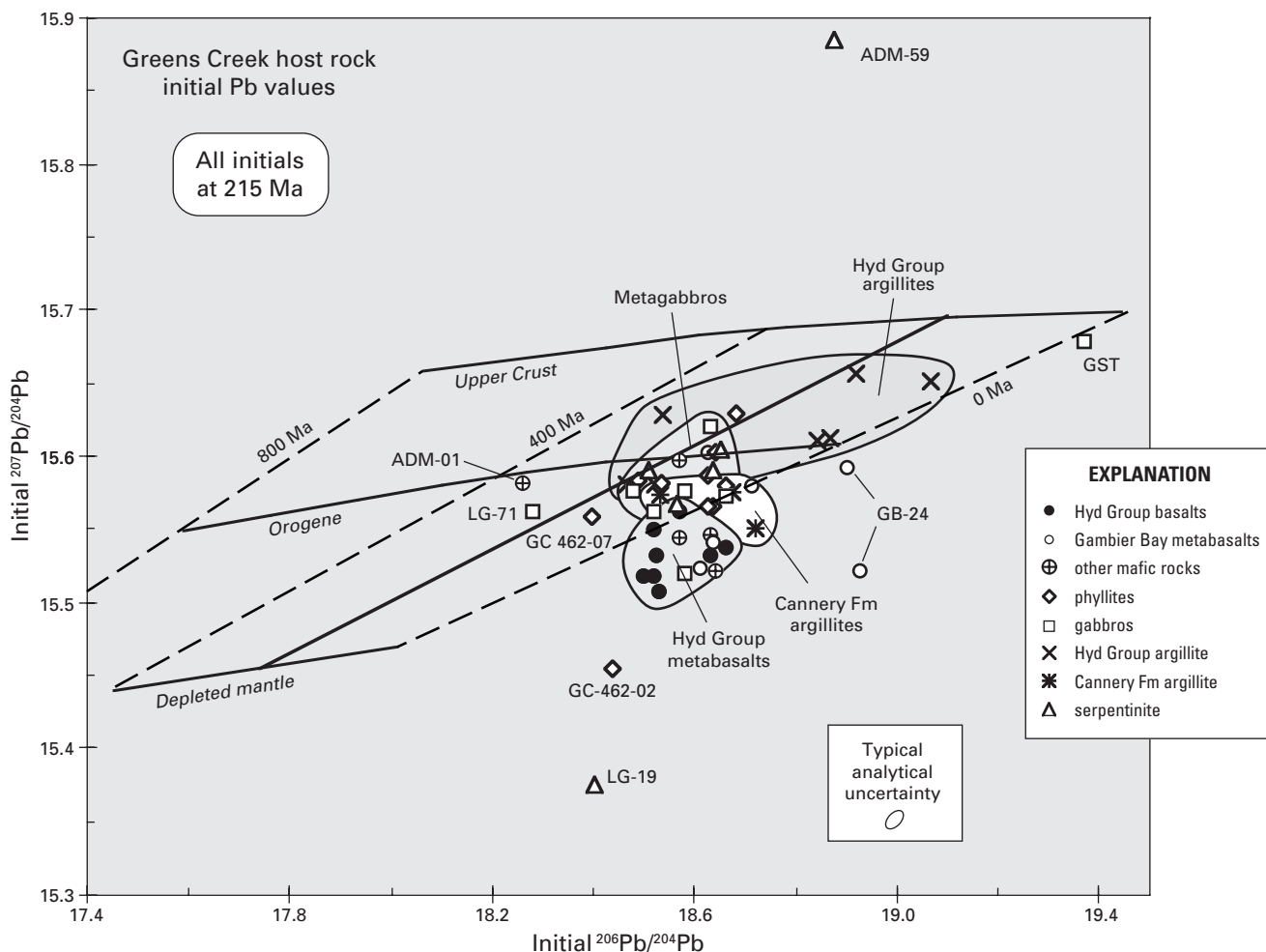


Figure 10. Pb-Pb correlation diagram ($^{206}\text{Pb}/^{204}\text{Pb}$ versus $^{207}\text{Pb}/^{204}\text{Pb}$) showing the distribution of initial Pb compositions of Greens Creek host rocks relative to model lead evolution curves and fields for modern petrotextonic environments (Zartman, 1984). Most mafic lithologies have initial lead values (at 215 Ma) between the “orogene” and “depleted mantle” curves, however, plotting at younger model lead ages (dashed isochrons). Scatter in the isotopic data may be due to postemplacement U-Pb fractionations caused by either low-grade metamorphism or subsequent alteration, particularly within the metagabbros. The field defined by metabasalts, largely those of the Hyd Group, is more discrete (less variation), plotting midway between the “orogene” and “depleted mantle” curves. Their altered equivalents, the phyllites plot just to the left, implying slight U-Pb fractionations during alteration. Argillites also define a wide field (see text for discussion) but basically plot at or near the “orogene” and trending toward the “upper crust” curve, suggesting some older, more radiogenic crustal input.

advantage is that evaluation of lead isotopic data in comparison to them is more definitive. Henceforth, lead isotopic data from Greens Creek will be displayed and discussed mainly using the $^{206}\text{Pb}/^{204}\text{Pb} - ^{207}\text{Pb}/^{204}\text{Pb}$ correlation diagram.

Notably, all fields of initial $^{206}\text{Pb}/^{204}\text{Pb} - ^{207}\text{Pb}/^{204}\text{Pb}$ values at 215 Ma for Greens Creek host rocks do not plot on model lead compositions at the 200-Ma isochron (fig. 10). Nearly all of these initial lead values plot beyond — to younger model ages, indicating derivation from sources more enriched than average model reservoirs — and cluster nearer to the orogene curve than

to either of the other two curves. This lead isotopic behavior is not unusual for arc-related VMS deposits, as pointed out by Newberry and others (1997), and discussed further by Kerrick (1991) and Dickin (1995).

Also, there are profound differences between the $^{206}\text{Pb}/^{204}\text{Pb} - ^{207}\text{Pb}/^{204}\text{Pb}$ correlation (U-derived only) and the $^{206}\text{Pb}/^{204}\text{Pb} - ^{208}\text{Pb}/^{204}\text{Pb}$ correlation (or lack thereof). In figure 11, model lead evolution curves for “mantle,” “orogene,” and “upper crust” are subparallel and adjacent such that initial $^{206}\text{Pb}/^{204}\text{Pb} - ^{208}\text{Pb}/^{204}\text{Pb}$ signatures from Greens Creek host

rocks overlap both the upper crust and the orogene model lead evolution curves. However, the data do mainly cluster about the upper-crust model lead curve, and are unlike lead signatures for either the lower crust or a depleted mantle.

Metabasalts

Although the lead contents in the metabasalts are more variable (2 to 12 ppm), the uranium contents are between 0.2 and 1 ppm, and thorium between 0.5 and 3 ppm (table 4, chap. 11) typical of modern-day basalts. Two exceptions, LG-17 and GB-24, are much more depleted and exhibit uranium and thorium concentrations similar to ultramafic rocks and Greens Creek serpentinite.

The U-Pb isotopic data for the Hyd Group metabasalts define an apparent isochron age of 218 ± 16 Ma with initial leads value of 18.515 (fig. 11; chap. 11) that, while not very precise, lends confidence to their calculated initial lead signatures at 215 Ma. These metabasalts (and related phyllites – altered mafic volcanics) plot between average lead compositions for “orogene” and “mantle,” consistent with their derivation from mainly mantle sources (fig. 10) but probably in a volcanic arc setting (Zartman and Doe, 1981; Zartman, 1984). Initial lead values for the Hyd Group metabasalts (mainly from Gambier Bay; fig. 3) plot within the metagabbroic/ultramafic field, but in a much more discrete area, perhaps indicative of their higher degree of preservation and isotopic stability. A notable exception, two analyses of metabasalt GB-24 plot to

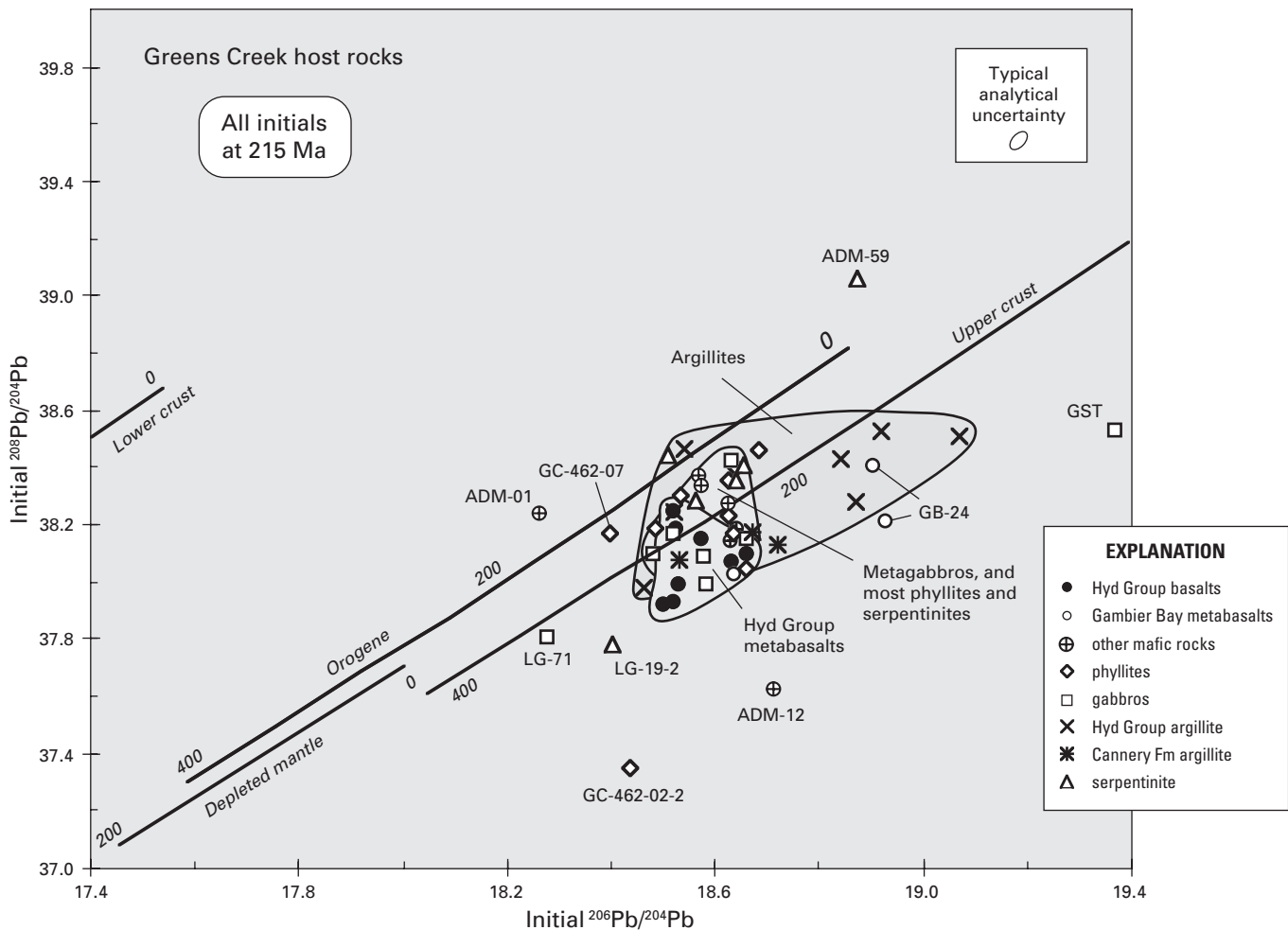


Figure 11. Pb-Pb correlation diagram ($^{206}\text{Pb}/^{204}\text{Pb}$ versus $^{208}\text{Pb}/^{204}\text{Pb}$) showing the distribution of initial lead compositions of Greens Creek host rocks relative to model lead evolution curves and fields for modern petrotectionic environments (Zartman, 1984). Model lead evolution curves for “mantle,” “orogene,” and “upper crust” are subparallel and adjacent such that modern-day isotopic fields for petrotectionic environments (for example, OIB, MORB, IAB) overlap grossly. Initial lead signatures from Greens Creek host rocks unfortunately overlap two of the model lead evolution curves and therefore are not uniquely interpretable using these model lead discriminators.

the right with a higher $^{206}\text{Pb}/^{204}\text{Pb}$ relative to the other Gambier Bay Formation metabasalt (figs. 10 and 11).

Rubidium and strontium concentrations in metabasalts vary widely and apparently are not correlated with degree of alteration or metamorphism (tables 3 and 6). Typical unaltered basalts have Rb contents around 30 ppm and relatively high Sr contents (about 450 ppm) due to their more calcic mineral assemblages. Greens Creek metabasalts have variable Rb (3 – 41 ppm) and low average Sr (125 – 250 ppm) contents, indicating either derivation from a less mafic source or mobility during subsequent metamorphism and/or alteration. A metabasalt, GB-24, from the Gambier Bay Formation is altered and exhibits extremely depleted Rb-Sr contents, similar to serpentinites. Two other metabasalts, GB-42 and GB-55, have high Sr contents (540 – 700 ppm). High Sr contents (>600 ppm) are indicative of carbonates.

Samarium and neodymium contents from the metabasalts are much less scattered (2–5 ppm and 5–21 ppm, respectively; table 6 in chap. 11) and are typical of tholeiites, although slightly more enriched than MORB and less enriched than continental tholeiites (for example, Faure, 1986). Metabasalt, LG-17, from Gallagher Ridge (fig. 5) is highly altered and exhibits more depleted Sm-Nd contents (0.7 and 3 ppm, respectively).

Sm-Nd isotopic data for the Hyd Group metabasalts define an apparent isochron age of 215 ± 95 Ma (fig. 12, chap. 11) and, while not very precise, they do indicate that calculated initial neodymium signatures at 215 Ma are accurate. The Rb-Sr isotopic data for the same suite of Hyd Group metabasalts are not as well defined, but two separate arrays indicate ages at about 190 to 170 Ma but with slightly different initial strontium values of 0.7041 and 0.7049 (fig. 13; chap. 11). Therefore, their calculated initial strontium values are probably slightly lower than they should be. However, this small difference does not alter any of our interpretations regarding the Rb-Sr isotopic systematics for these metabasalts.

With respect to their Nd-Sr isotopic systematics, the metabasalts can be subdivided into at least two groups: a high-Nd ($\epsilon_{\text{Nd}} = +7$ to 9) group that includes most Hyd Group metabasalts from Gambier Bay, southeastern Admiralty Island (fig. 3), and a lower-Nd ($\epsilon_{\text{Nd}} = +4$ to 5) group (fig. 12). Some of the high-Nd metabasalts exhibit low-Sr values (for example, GB-42; $^{87}\text{Sr}/^{86}\text{Sr}_i$ about 0.704), whereas, others have more elevated Sr values ($^{87}\text{Sr}/^{86}\text{Sr}_i = 0.7049$ to 0.7056), possibly due to alteration. Samples GB-24 and GB-80 are in this category. Lower Nd and lower Sr values ($\epsilon_{\text{Nd}} = +4$ to 5, and $^{87}\text{Sr}/^{86}\text{Sr}_i = 0.07038$, respectively) are exemplified by sample GB-55, a chloritized greenstone from the Gambier Bay Formation at Gambier Bay, and a similarly lower-Nd metabasalt, GB-59, has an elevated Sr value ($^{87}\text{Sr}/^{86}\text{Sr}_i$ about 0.7043). Other lower-Nd metabasalts include LG-17 from Gallagher Ridge ($\epsilon_{\text{Nd}} = +5$) and ADM-12 ($\epsilon_{\text{Nd}} = +4.3$) from Staunch Point (fig. 3). Although this last sample is described as a microgabbro (table 3), it is highly altered and could have a basaltic protolith.

All of the metabasalt data lie well within the modern “island arc” field with elevated $^{87}\text{Sr}/^{86}\text{Sr}$ relative to OIB or

MORB (fig. 12). Time-corrected values (at 215 Ma) for the OIB and MORB fields plot slightly farther to the left in the diagram, enhancing the difference between initial Nd-Sr values for Greens Creek samples and those for different petro-tectonic environments at 215 Ma.

A comparison of initial neodymium and lead (fig. 13) for Greens Creek metabasalts is even more discrete than that for Nd-Sr initial signatures. Lower-Nd metabasalts are also characterized by slightly higher average initial $^{206}\text{Pb}/^{204}\text{Pb}$ values than the more depleted, high-Nd metabasalts. Elevated initial $^{206}\text{Pb}/^{204}\text{Pb}$ values relative to MORB and OIB like $^{87}\text{Sr}/^{86}\text{Sr}$ are indicative of some modern oceanic island arc settings (for example, Ellam and Hawkesworth, 1988; Ben Othman and others, 1989). Again, metabasalt GB-24 is notably an outlier with a significantly higher initial $^{206}\text{Pb}/^{204}\text{Pb}$ value similar to serpentinite, ADM-59 (fig. 13).

Metagabbros

Metagabbro lead contents are depleted (less than 1 ppm) relative to metabasalt values, as are uranium contents (0.08–0.5 ppm) and thorium (0.25–2.5 ppm). All of these concentrations are at least half as depleted relative to typical, modern-day values for gabbro (for example, Faure, 1986). Th/U ratios are relatively uniform at about 3.3; a highly altered, massive microgabbro, LG-45, is the only exception.

The U-Pb isotopic data for the metagabbro data define an apparent isochron age of 206 ± 35 Ma indicating an initial $^{206}\text{Pb}/^{204}\text{Pb}$ value of 18.61 (fig. 14; chap. 11) and again, while not very precise, these results do lend confidence in the calculated initial lead signatures at 215 Ma for these metagabbros.

The wide array of initial Pb values for metagabbros and serpentinites more than likely represents slight, yet significant U/Pb fractionations since their emplacement and crystallization. It should be noted, however, that average composition(s) for metagabbroic-serpentinitic magmatic source(s) are very similar to those for metabasalts and phyllites and lie between the “mantle” and “orogene” averages (fig. 10), again indicative of their partial derivation from a depleted mantle source.

Rb-Sr contents for the metagabbros (0.5–23 and 120–330 ppm, respectively) are lower and less scattered than those for the metabasalts, and most lie along a Rb/Sr trend of about 0.01; the highly altered metagabbros, LG-45 and LG-71, are the only exceptions. Samarium and neodymium concentrations (1–4.5 and 3–16 ppm, respectively), like Rb-Sr, are on average lower than those for metabasalts and more similar to typical average modern-day MORB concentrations.

Sm-Nd isotopic data for the Greens Creek metagabbros define an apparent isochron age of 200 ± 27 Ma (fig. 15; chap. 11) and, while not very precise, they do indicate that calculated initial neodymium signatures at 215 Ma are accurate.

Metagabbros plot between the two groups of metabasalt (figs. 12 and 13) with initial $\epsilon_{\text{Nd}} = +5$ to 7, initial $^{87}\text{Sr}/^{86}\text{Sr} = 0.07037$ to 0.7048, and initial $^{206}\text{Pb}/^{204}\text{Pb} = 18.45$ to 18.66, slightly more depleted than the lower-Nd metabasalts and slightly more enriched than the high-Nd metabasalts.

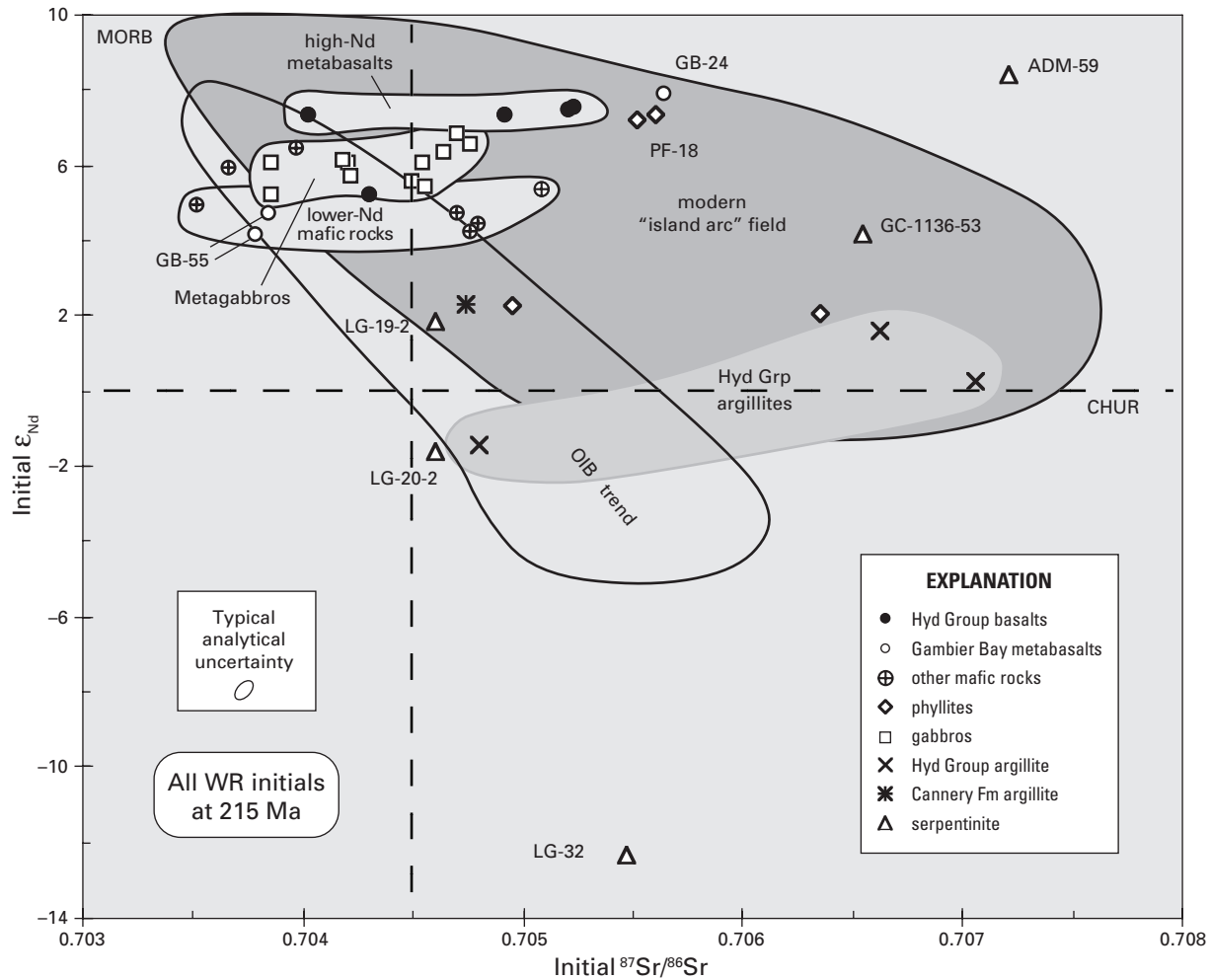


Figure 12. Initial strontium versus initial neodymium correlation diagram showing the distribution of initial Sr-Nd values for Greens Creek host rocks relative to model Sr-Nd fields for modern petro-tectonic environments (for example, Zartman, 1984). Again, most initial Sr-Nd data for these host rocks plot between mid-ocean ridge basalt (MORB) and more enriched values, and mostly displaced to the right in the “island-arc” field relative to the oceanic-island basalt (OIB) trend. Serpentinite data vary widely. See text for more discussion. CHUR, chondritic uniform reservoir.

Initial Sr and Nd values (at 215 Ma) for mafic igneous rocks from Greens Creek have higher ϵ_{Nd} (+4 to +9) and lower $^{87}Sr/^{86}Sr$ (0.7035 to 0.7058) than phyllites and argillites, values indicating mainly mantle derivation (fig. 12). All samples are enriched in $^{87}Sr/^{86}Sr$ and $^{206}Pb/^{204}Pb$ compared to MORB (mid-ocean ridge basalt) or OIB (oceanic island basalt), a characteristic indicative of island arc rocks (Hawkesworth and others, 1977, 1979; Zartman, 1984; Ellam and Hawkesworth, 1988; Ben Othman and others, 1989). Metagabbro LG-71 and metabasalt ADM-01 plot to the left with unusually low $^{206}Pb/^{204}Pb$ values of about 18.27 (fig. 13). We suspect that the U-Th-Pb isotopic systematics from these whole-rock samples may be disturbed (fig. 7A), and caution is advised to the reader regarding some of these data.

Phyllites

Uranium, thorium, and lead concentrations for phyllites (0.1–2 ppm, 0.4–9.3 ppm, and 4–100 ppm, respectively) have a much broader range than the metabasalts, their less altered equivalents. On average, however, the phyllite concentrations are not significantly different. One sample, GC-462-02-2, produced an unusually high thorium concentration of 9.3 ppm; otherwise, thorium contents range between 0.4 and 2.4 ppm. Lead contents from two mine phyllites, GC-1103-16 and GC-1637-44, were uncharacteristically high (60 and 98 ppm, respectively); otherwise, the lead contents ranged between 4 and 13 ppm, almost exactly that of the metabasalts. Th/U ratios for phyllites are variable and typically have lower values than the main mafic trend of about 3.3 (with the exception of PF-18).

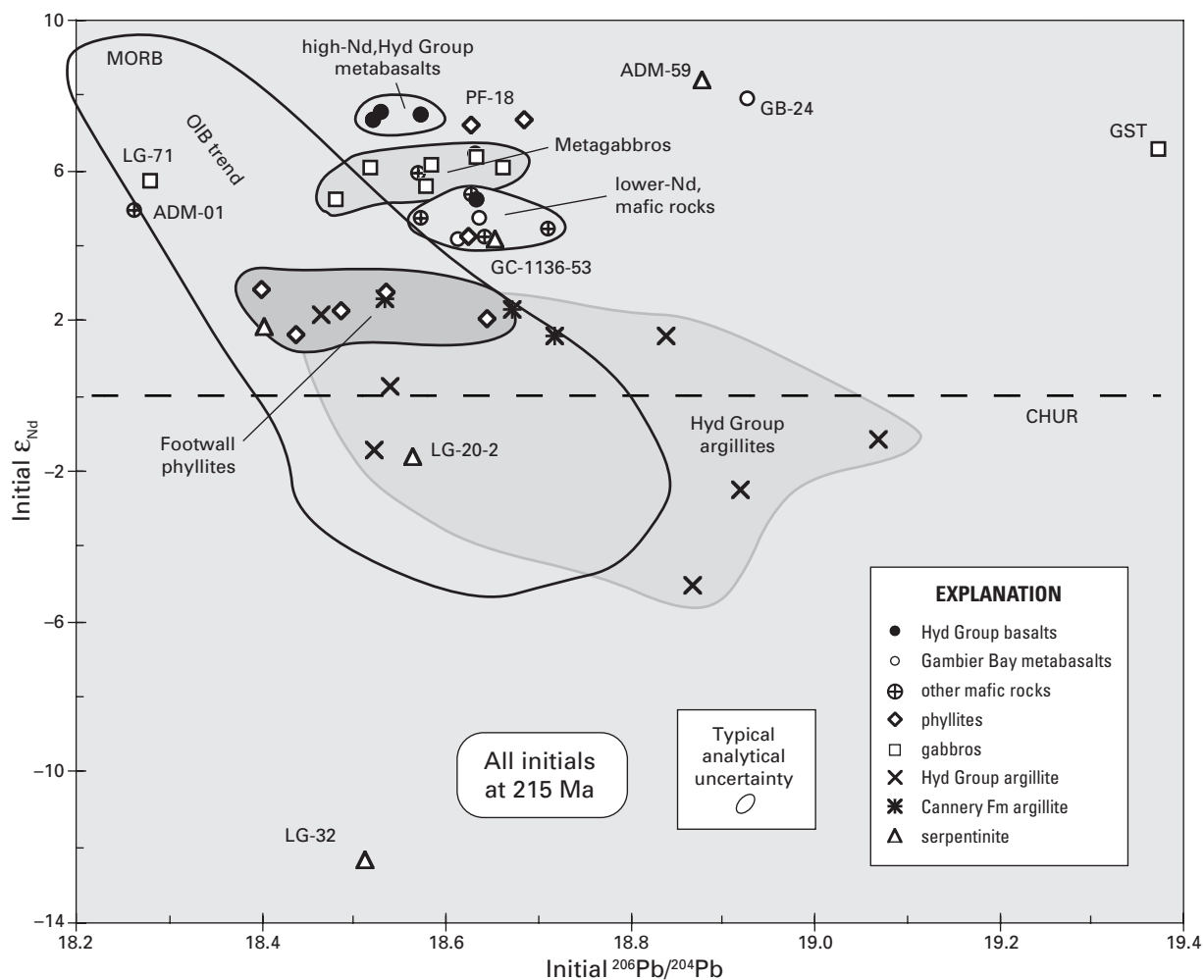


Figure 13. Initial lead versus initial neodymium correlation diagram showing the distribution of initial Pb-Nd values for Greens Creek host rocks relative to model Pb-Nd fields for modern petrotectonic environments (for example, Zartman, 1984). Fields representing different lithologic units of Greens Creek host rocks are more discrete than those shown in figure 12, and a field for most of the phyllites is somewhat discernible from values for argillites. Although a field for modern “island arcs” is not shown, elevated $^{206}\text{Pb}/^{204}\text{Pb}$ values for most Greens Creek mafic rocks relative to the ocean-arc basalt (OIB) trend is indicative of some modern island-arc rock suites (Ellam and Hawkesworth, 1988; Ben Othman and others, 1989). Again, serpentinite data vary widely (although ADM-59 is joined by metabasalt GB-24). MORB, mid-ocean ridge basalt; OIB, oceanic-island basalt; CHUR, chondritic uniform reservoir.

The phyllites, interpreted as altered mafic volcanic rocks, exhibit initial Pb isotopic compositions similar to the meta-basalt and metagabbro initial Pb compositions (figs. 10 and 11), although more scatter is evident — an indication of U-Pb fractionations during subsequent alteration (fig. 11, chap. 11). Although the phyllites plot mostly within the metagabbro field, this field significantly overlaps fields for both the metabasalts and the argillites.

Rubidium and strontium concentrations vary somewhat (1–55 ppm and 26–112 ppm, respectively), notably lower in strontium and slightly higher in rubidium contents than associated metabasalts, perhaps due to alteration. Samarium and neodymium contents are less variable (0.6–4.4 ppm and 3–18.4 ppm, respectively) and very similar to their less-altered equivalents, the metabasalts.

Although the calculated initial lead values for phyllite samples mimic those of the metabasalts and metagabbros, calculated initial Sr-Nd and Pb-Nd values of phyllites are more scattered (figs. 12 and 13). The difference in initial strontium in phyllites can be explained by alteration due to seawater interaction or incorporation of carbonate ($^{87}\text{Sr}/^{86}\text{Sr} = 0.707$ to 0.708), as is probably the case with some of the argillites, metabasalts, and serpentinites. Two phyllites (PF-09 and GC-1637-44) plot with very low initial strontium values (less than 0.703) are not within the scale of the diagram (fig. 12), and are suspected of containing secondary rubidium (see fig. 7B). Two analyses of phyllite PF-18 from the Portal Face are similar to the high-Nd metabasalt signature ($\epsilon_{\text{Nd}} = +8$), but with slightly more enriched strontium (0.7056) and lead (18.67) signatures. Other phyllites

plot toward initial signatures for argillites with ϵ_{Nd} about +2, higher initial strontium and lower initial lead, consistent with their lower Th/U, increased uranium content (leading to over-corrected initial lead values).

Differences in initial neodymium are not easily explained or well understood. Because the initial neodymium values of some phyllites tend toward values for argillites, one might suggest that hydrothermal fluids circulating through both the argillitic and older mafic volcanic packages (phyllites) mobilized rare-earth elements (REE) and therefore altered neodymium compositions. Nevertheless, lower ϵ_{Nd} and higher $^{87}\text{Sr}/^{86}\text{Sr}$ values in some Greens Creek samples probably indicate the addition of older, more enriched crustal components either during sedimentation or subsequent alteration (figs. 7 and 8).

Argillites

Argillite samples are of two known ages: an older Permian suite from the Cannery Formation (LG-78, ADM-29, and ADM-34), and a younger, Late Triassic, Greens Creek-contemporary suite from the Hyd Group sequence (table 3, chap. 11). A comparison of uranium, thorium, and lead concentrations from the two suites reveals no differences (0.7–4, 0.2–4.5, and 1.7–20 ppm, respectively), nor do Th/U ratios show any distinction. As mentioned previously, the variations in Th/U would suggest variable fractionation either during shale deposition or subsequent alteration. Unusually high uranium contents were found in mine argillite PP-204-01 (7.4 ppm).

The argillites yielded an apparent U-Pb isochron age of 186 ± 100 Ma (chap. 11), and whereas this age is very imprecise, if accurate, it is interestingly similar to U-Pb and Rb-Sr apparent isochron ages for some of the metabasalts and phyllites (about 205 and 182 Ma, respectively) and ages of either intrusion or alteration of the metagabbros (about 206 Ma). Despite slight alteration, these isochron ages lend confidence to calculated initial Pb signatures at 215 Ma for the argillite samples.

On average, a higher ^{207}Pb component can be found in initial lead compositions from some of the argillites (fig. 10). These values range from average “orogene” to “upper crust” compositions, indicating that lead in some of the argillites is derived from an older, slightly more radiogenic source. The same indication is observed in ^{206}Pb – ^{208}Pb space (fig. 11) — argillites plot approximately on the model “upper crust” Pb evolution curve at 200 Ma.

Argillite Pb signatures can be subdivided into two fields (see fig. 15, chap. 10). The least radiogenic argillite field is compatible with some phyllites, but also galena Pb from Kennecott-Rand. And the most radiogenic argillite field appears as a possible endmember composition consistent with some Greens Creek pyrite and sphalerite Pb compositions. In general, the older Cannery Formation argillites plot under the Hyd Group argillites (lower $^{206}\text{Pb}/^{204}\text{Pb}$ and $^{207}\text{Pb}/^{204}\text{Pb}$) and within the upper section for the metabasalts and phyllites. The Hyd Group argillites, on the other hand, plot either to the low $^{206}\text{Pb}/^{204}\text{Pb}$ side, similar to values for galena Pb from Kennecott-Rand, some phyllites and some metagabbros, or to the

high $^{206}\text{Pb}/^{204}\text{Pb}$ side, similar to some Greens Creek pyrite and sphalerite Pb compositions that may contain more evolved, younger lead (Cretaceous pyrite formation?).

Rb-Sr concentrations from argillites vary widely (1–60 ppm and 1–135 ppm, respectively), although in general Rb/Sr ratios are quite high (0.2–20). These concentrations are considerably below the typical average shale concentrations for Rb and Sr (about 140 and 300 ppm, respectively). Sm-Nd contents in typical modern shales are 10 and 50 ppm, respectively (for example, Faure, 1986), far greater than those exhibited by Greens Creek argillites (0.7–4 ppm and 3.2–18.2 ppm, respectively); however, Greens Creek argillites have Sm-Nd contents near exactly the same as associated phyllites and metabasalts from which they were supposedly derived.

Rb-Sr isotopic age data for the argillite samples suggest a single resetting age of 91.4 ± 2.6 Ma (fig. 16, chap. 11) that includes Hyd Group and Cannery Formation alike. It is essentially a three-point isochron controlled by two Hyd Group argillites, LG-66 and NAD-T4-2, neither of which is carbonaceous. Omission of the Cannery Formation data alters the Rb-Sr apparent isochron age to 90.8 ± 2.2 Ma with initial $^{87}\text{Sr}/^{86}\text{Sr}$ at 0.70733 for the Hyd Group argillites, a value that approaches Cretaceous seawater strontium composition (figs. 7 and 8).

Correctable initial Nd-Sr-Pb isotopic data for argillites (only four analyses) lie in fields with lower initial Nd (ϵ_{Nd} about –2 to +2), higher initial $^{206}\text{Pb}/^{204}\text{Pb}$ (18.45–19.08), and higher initial $^{87}\text{Sr}/^{86}\text{Sr}$ (0.7048 to 0.7070) than other host rocks (figs. 12 and 13), but typical of values for modern shales (between modern OIB and “orogene”). High ^{207}Pb , low ϵ_{Nd} , and higher Sr values all suggest that the argillites contain older, slightly more radiogenic source material, perhaps indicative of some Paleozoic provenance (Alexander terrane). However, because these Sr-Pb isotopic data may have been altered, even slightly (figs. 7 and 8), an emphasis on the initial Nd values is recommended. Nonetheless, the initial Pb-Sr-Nd isotopic signatures for argillites do plot on average where one might expect from the interpreted tectonic setting — an oceanic arc environment (for example, Zartman, 1984).

Serpentinities

Uranium, thorium, and lead contents in ultramafic rocks average 0.015, 0.05, and 0.3 ppm, respectively, and Greens Creek serpentinites exhibit comparable concentrations of 0.01–0.06, 0.03–0.2, and 0.2–0.75 ppm, respectively. Several outliers are observed; ADM-59 is exceptional with uranium (0.11 ppm), thorium (0.95 ppm), and lead (4.7 ppm); and mine serpentinites GC-1136-53 and GC-1136-59 are enhanced with uranium and lead (0.04–0.07 and 75–26 ppm, respectively). The high lead contents in the latter two are indicative of alteration due to mineralization, and these lead results should therefore be ignored when evaluating the isotopic systematics of the serpentinites.

The initial lead compositions for most serpentinites lie within the mafic igneous field (fig. 10). However, two exceptions exist: an extremely low $^{207}\text{Pb}/^{204}\text{Pb}$ analysis of LG-19-2 and an extremely high $^{207}\text{Pb}/^{204}\text{Pb}$ analysis of ADM-59.

Because of large errors (table 4, chap. 11) and the possibility of difficulties in maintaining stable $^{207}\text{Pb}/^{204}\text{Pb}$ measurements relative to $^{206}\text{Pb}/^{204}\text{Pb}$ (see chap. 10), these two serpentinite analyses are highly tentative. Nonetheless, if these results are even somewhat accurate, they do present interesting speculation.

Typical ultramafic rubidium and strontium concentrations are 0.2 and 1 ppm, respectively, and Greens Creek serpentinites range between 0.15 and 0.32, and 6.8 and 16 ppm, respectively (table 6, chap. 11). Exceptions are noted with mine serpentinites GC-1136-53 and GC-1136-59 that exhibit extreme Rb and Sr contents of 33 to 45 and 68 to 153 ppm, respectively, and these analyses again should be excluded when considering the Rb-Sr isotopic characteristics of the serpentinite protolith(s). Samarium and neodymium concentrations for typical modern ultramafic rocks vary, but generally are below 0.6 and 2.5 ppm, respectively. Greens Creek serpentinites range between 0.017–0.03 and 0.09–2.7 ppm, respectively, excluding the mine serpentinites (table 6, chap. 11).

Although the Rb-Sr isotopic data from serpentinite samples are scattered and do not form well-defined isochrons, an age of about 195 Ma is suggested for serpentinites LG-19 and LG-20 from the Lakes District area (fig. 5), probably an age close to that of alteration. An initial Sr value of 0.70462 ± 6 is calculated from this regression, a value very similar to both metabasalts and some metagabbros (fig. 17, chap. 11).

Another Rb-Sr age of 89 ± 15 Ma (fig. 17, chap. 11) is defined by the two mine serpentinites, GC-1136-53 and GC-1136-59, with an initial Sr value of 0.70767 — a value very similar to that indicated by the data from the Hyd Group argillites (0.70733) with a Rb-Sr age of resetting at 91 Ma (fig. 16, chap. 11). Serpentinite ADM-59 from Gambier Bay plots near this “reset” isochron.

Initial Pb-Sr-Nd isotopic values for serpentinite vary widely (figs. 10 through 13) due in part to the poor quality of the analyses (very low abundances and correspondingly low ion beam intensities). If one can believe the data, however, they suggest highly variable source(s) during emplacement (perhaps over a substantial time period) or isotopic resetting during alteration probably due to Cretaceous deformation. An attempt to date serpentinite sample LG-19 was largely unsuccessful in all isotopic systems, indicating that internal isotopic systematics had been disturbed (chap. 11).

With the hope that any of these serpentinite analyses are accurate, if not precise, their isotopic behavior imply several interesting points. One of the serpentinites (ADM-59) is much different than the rest, with high initial Nd (+8.4), high $^{207}\text{Pb}/^{204}\text{Pb}$ (15.885), and high $^{87}\text{Sr}/^{86}\text{Sr}$ (0.7072), whereas the remainder of the serpentinites exhibit decreasing initial Nd values (GC-1136-53, +4.15; LG-19-2, +1.8; LG-20-2, -1.6; and so forth), indicating increasing crustal involvement in their production (figs. 9, 12, and 13). If these results are accurate, it would suggest that serpentinite LG-32, the most negative (ϵ_{Nd} about -12), was derived from a source enriched with much older crust (Nd model age, $T_{\text{DM}7} = 1,350$ Ma). Unfortunately, age data for any of these serpentinites do not exist; they may range anywhere in age from Late Triassic to Cretaceous.

Crosscutting Diabases — Diorites

Uranium, thorium, and lead contents for these samples are given in table 4 (chap. 11), initial Pb values are given in table 5 (chap. 11), and they indicate that these sills/intrusions are of two types. Samples LG-64 (diorite) and GC-1704-01 are remarkably similar, especially with respect to their Nd-Sr and Nd-Pb isotopic systematics (not shown), and GC-1701-01 is notably different. All of these samples have uranium contents between 0.84 and 1.35 ppm and thorium contents between 1.6 and 2.6 ppm, but variable lead contents of about 4 ppm to 640 ppm, the latter indicative of contamination by mineralization — sample GC-1701-01. Otherwise, the diabasic intrusions are similar to the metabasalts, metagabbros, and phyllites with respect to their U, Th, and Pb contents.

Without an actual age for these intrusions, accurate initial Pb compositions are not possible. All of these bodies are known to be younger than the Greens Creek ore-forming event, but how much younger has not been established. Assuming reasonably contemporaneous ages for these crosscutting intrusions (from 185 to 90 Ma), initial lead and strontium values do not match Cretaceous lead and strontium model isotopic compositions (for example, Burke and others, 1982; Zartman, 1984), suggesting that the isotopic systematics of these samples are not controlled by Cretaceous deformation and(or) seawater alteration. Initial Nd-Sr and Nd-Pb correlation diagrams (from 215 Ma to 50 Ma) show that these samples, and especially LG-64 and GC-1704-01, are quite similar and depleted; in fact, the most depleted whole-rock samples at Greens Creek had initial $\epsilon_{\text{Nd}} = +7$ to 8, $^{87}\text{Sr}/^{86}\text{Sr} = 0.7033$, and $^{206}\text{Pb}/^{204}\text{Pb} = 18.2$ to 18.45, values slightly less than MORB at 185 to 90 Ma.

Discussion

Geologic Framework at Greens Creek

We know from previous geologic studies that the Greens Creek ore deposit is located in a belt of volcano-sedimentary rocks interpreted to represent a rift-fill sequence formed during a brief period of intra-arc or back-arc rifting in latest Triassic time (Berg and others, 1972; Taylor, 1997; Taylor and others, 1995a, 1995b, 1999, 2000). The stratigraphy within the belt consists of conglomerates, limestones, marine clastic sediments, and tuffs that are intercalated with and overlain by a distinctive unit of mafic pyroclastics and pillowed flows (figs. 3 and 4). Faunal data bracket the age of the host rocks between early Carnian (early Late Triassic) and late Norian (late Late Triassic) time (chap. 11).

The radiogenic isotopic systematics indicate a progressively depleting source for the Upper Triassic Greens Creek rocks, suggesting a rift setting. The oldest argillites have slightly depleted signatures (ϵ_{Nd} about +1.5), consistent with their derivation from mainly oceanic-arc volcanic rocks of the Alexander terrane. These rocks in turn are unconformably overlain by a sequence of mainly altered metabasalts

and related rocks, perhaps similar to metabasalts of either the Halleck Formation or the Gambier Bay Formation that exhibit depleted, island-arc-type isotopic signatures (ϵ_{Nd} about +4 to 5 and elevated $^{87}Sr/^{86}Sr$ and $^{206}Pb/^{204}Pb$). The metabasalts are then unconformably overlain by conglomerate, dolomite, and more argillites of the Hyd Group. The Hyd Group argillites have slightly depleted to slightly enriched ϵ_{Nd} about -5 to +2, indicating partial incorporation of some older, more enriched source material. The lower metabasaltic sequences are intruded by ultramafic sills and stocks, represented now as highly altered serpentinites that exhibit a wide range of isotopic signatures (ϵ_{Nd} about -12 to +8), suggesting that they may have been early to late rift-forming intrusions, and enriched relative to other igneous rocks. Subsequent mafic volcanism and gabbroic plutonism are characterized by more depleted source signatures ($\epsilon_{Nd} = +5$ to +9). Hyd Group basalts that cap the Triassic section have yet more depleted signatures ($\epsilon_{Nd} = +8$ to +9), and lastly, post-Greens Creek crosscutting diabase dikes are the most depleted ($\epsilon_{Nd} = +9$). This progressive sequence of least to most depleted isotopic signatures implies opening of preexisting crust in a rift setting, most likely within an oceanic arc environment.

Petrotectonic Environment of the Greens Creek VMS Deposit

Scatter in the isotopic data for phyllites, metagabbros, serpentinites, and argillites indicate the likelihood of open-system behavior due to mobilization of either or both elements probably during Cretaceous deformation and metamorphism. However, despite this probable isotopic behavior, average initial Pb-Sr-Nd isotopic data from the mafic rock units (metabasalts, metagabbros, and associated phyllites) plot where one might expect them and indicate derivation from sources similar to those of oceanic-arc environments. Initial Pb signatures for the basaltic-gabbroic-ultramafic magmatic source(s) and related phyllites (altered mafic volcanics?) plot between average Pb compositions for “orogene” and “mantle,” consistent with their derivation from mainly mantle sources (fig. 10), but in a volcanic arc setting (Zartman and Doe, 1981; Zartman, 1984). Likewise, initial Sr and Nd (at 215 Ma) values for mafic igneous rocks from Greens Creek are depleted (higher ϵ_{Nd} and lower $^{87}Sr/^{86}Sr$), indicating mainly mantle derivation (fig. 12). All samples are enriched in $^{87}Sr/^{86}Sr$ and $^{206}Pb/^{204}Pb$ compared to MORB (mid-ocean ridge basalt) or the OIB (oceanic island basalt) trend, a characteristic indicative of island-arc rocks (Hawkesworth and others, 1977, 1979; Ellam and Hawkesworth, 1988; Ben Othman and others, 1989). Explanations for the elevated Sr values include the addition of subducted ^{87}Sr from seawater and/or oceanic sediments (Hawkesworth and others, 1977), or metasomatic contamination of the mantle wedge with high $^{87}Sr/^{86}Sr$ derived from subducted ocean crust (Pearce, 1983). Although some of these enriched values may be the result of alteration during Cretaceous deformation, even the most depleted values are slightly more enriched than MORB values.

Initial Nd values for phyllites are bimodal; some have a mafic igneous signature (+8), others trend toward initial signatures for the argillites (+2). Argillites tend to have lower Nd (ϵ_{Nd} about -5 to +2) and higher $^{87}Sr/^{86}Sr$ (0.705 to 0.707) than other host rocks and serpentinite data scatter widely, partly due to the questionable quality of the analyses, but also because of post-emplacement alteration. High ^{207}Pb , low ϵ_{Nd} , and higher Sr values all suggest that the argillites contain older, slightly more radiogenic, crustal material, perhaps indicative of a partial Paleozoic provenance. Crosscutting diabase dikes have variable Pb and Sr, but high ϵ_{Nd} values indicate that these dikes are from a depleted source — one sample exhibiting the most depleted isotopic signature of any of the Greens Creek host rocks.

Initial Nd-Sr isotopic signatures for Greens Creek host rocks are compared with other Nd-Sr isotopic results from Alexander and Gravina terranes (fig. 14) that have been interpreted to represent depleted, mantle-derived, oceanic island-arc environments (Samson and others, 1989, 1991a). Initial Nd isotopic compositions for Greens Creek metabasalt and metagabbro are similar to both Alexander and Gravina mafic rock data but vary more widely in Sr isotopic composition. This deviation could be the result of alteration and/or mobilization of Rb and Sr during Cretaceous deformation. Greens Creek argillite and serpentinite signatures vary widely, not unlike values from Alexander and Gravina metasedimentary samples. Sr values for other Alexander terrane samples (Samson and others, 1989) also approach Cretaceous seawater values (about 0.7078).

Interestingly, Alexander terrane felsic igneous rocks are more depleted (higher initial Nd and lower initial Sr) than their relatively coeval mafic counterparts. Two crosscutting bodies in the Greens Creek area, GC-1704-01 and LG-64, plot with the Alexander terrane felsic igneous rocks (fig. 14). A third dike, GC-1701-01, however, does not, but instead plots with the mafic igneous rocks. There were no other samples analyzed that come close to isotopic signatures exhibited by the serpentinites ADM-59 or LG-32, throwing further doubt on their validity.

Initial Lead Isotopes of Greens Creek Host Rocks Compared to Ore Lead Compositions

Lead isotopic data were obtained from many samples of galena, pyrrargyrite, sphalerite, pyrite, chalcopyrite, and tetrahedrite from inside the Greens Creek mine as well as several samples from outside the mine. Their lead isotopic compositions varied only slightly along a ^{207}Pb trend (fig. 11, chap. 10) and were compared to model lead evolutions for different large-scale, global sources or reservoirs (for example, mantle, orogene, upper crust; Zartman and Doe, 1981). The Greens Creek ore lead compositions ($^{206}Pb/^{204}Pb = 18.6-18.8$ and $^{207}Pb/^{204}Pb = 15.55-15.68$) plotted along the “orogene” evolution curve at a model lead age between 0 and 100 Ma. Some lead compositions lie along a high- ^{207}Pb trend, suggesting mixing with older, more radiogenic material, not unlike lead that could be derived from the Paleozoic Alexander terrane.

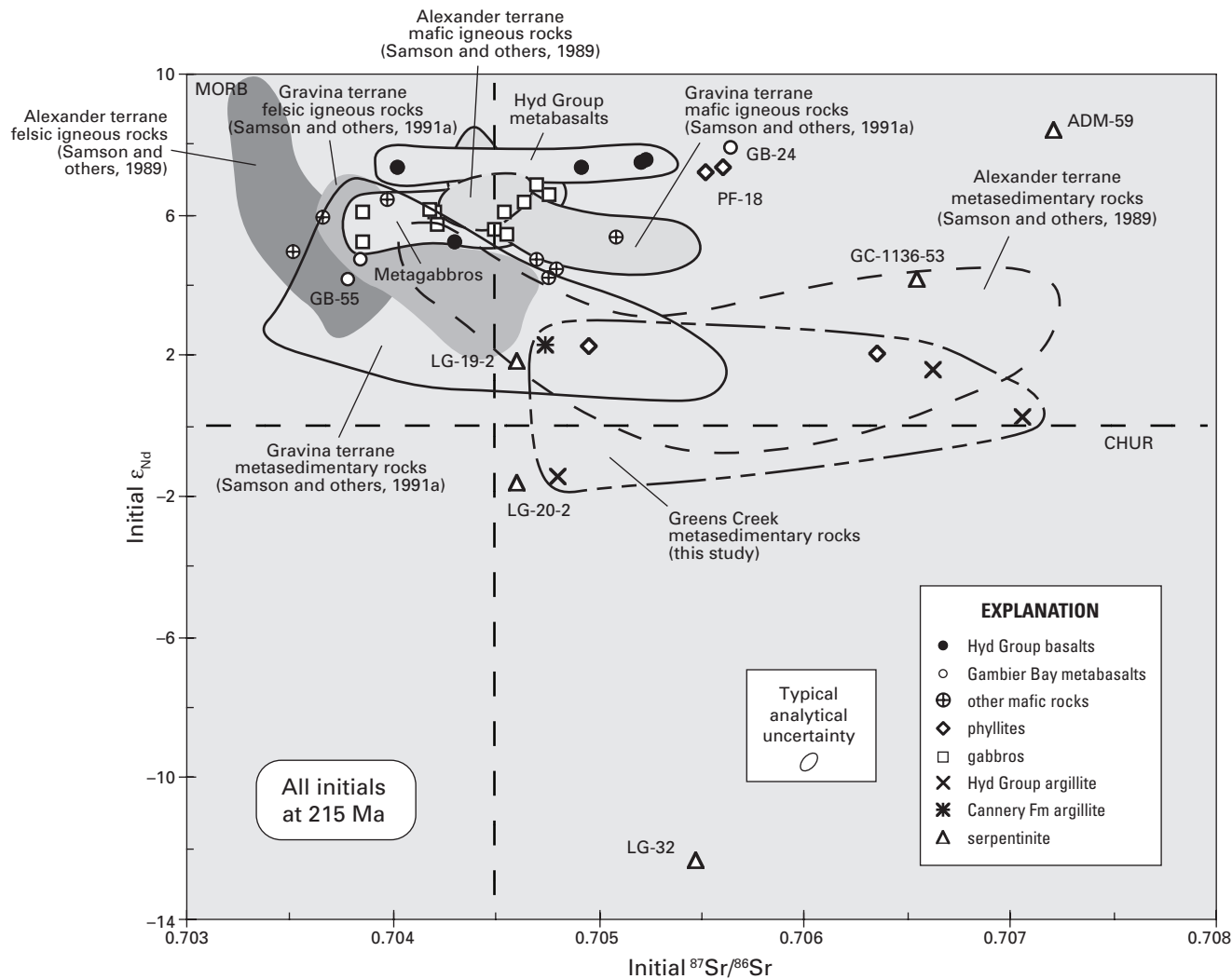


Figure 14. Initial strontium versus initial neodymium correlation diagram showing the distribution of initial Sr-Nd values for Greens Creek host rocks relative to Sr-Nd fields for previously published Alexander and Gravina terrane rocks (Samson and others, 1989, 1991a). Initial isotopic values for Greens Creek host rocks are more scattered than data shown for comparable lithologies of Alexander and Gravina terrane rocks; however, in general, the fields are not too dissimilar with relatively equal initial ϵ_{Nd} values for mafic lithologies and on average equal $^{87}Sr/^{86}Sr$ values. There are no felsic igneous rock data from Greens Creek to compare with the other terranes (except perhaps LG-64), but metasedimentary rock data from Greens Creek are very similar to that reported for other Alexander terrane metasedimentary samples. Again, data from serpentinites do not match any other results from either terrane, supporting the idea that these analyses are not reliable. MORB, mid-ocean ridge basalt; CHUR, chondritic uniform reservoir.

Likewise, initial lead isotopic compositions for host rocks have been compared to model lead compositions to help delineate their petrotectonic derivation (figs. 10 and 11). More important, initial lead compositions can be calculated to match the assumed age of mineralization (215 Ma), such that ore lead compositions can be directly compared to host/source-rock initial lead compositions to evaluate their genetic link, if any (fig. 15). A direct comparison such as this is a powerful tool in determining whether ore is syngenetic or epigenetic.

Lead isotopic data for Greens Creek ore suggest that it was formed through mixing between two main components: mafic magmatic source(s) represented by compositions of the metabasalts, metagabbros, and serpentinites, and compositions

given by the hanging-wall, pyritic, black argillites (fig. 15). The ore Pb field plots at the top of the mafic igneous fields, but not within it. Initial lead values for the various black argillites appear to embody the range of Pb values for the Greens Creek ore, suggesting that the ore Pb may be a homogenization of argillite Pb alone. On closer inspection, Pb values for unmineralized phyllites and argillites do not actually lie within the ore Pb field, but surround it (figs. 10 and 15). Therefore, it would appear that the Pb isotopic composition for Greens Creek ore is unique, and no particular host rock consistently shares that same composition. It is evident that the relatively uniform ore Pb signature may represent a homogenization of Pb derived from host metabasalt, metagabbro, some footwall phyllites, and the hanging-wall argillite(s).

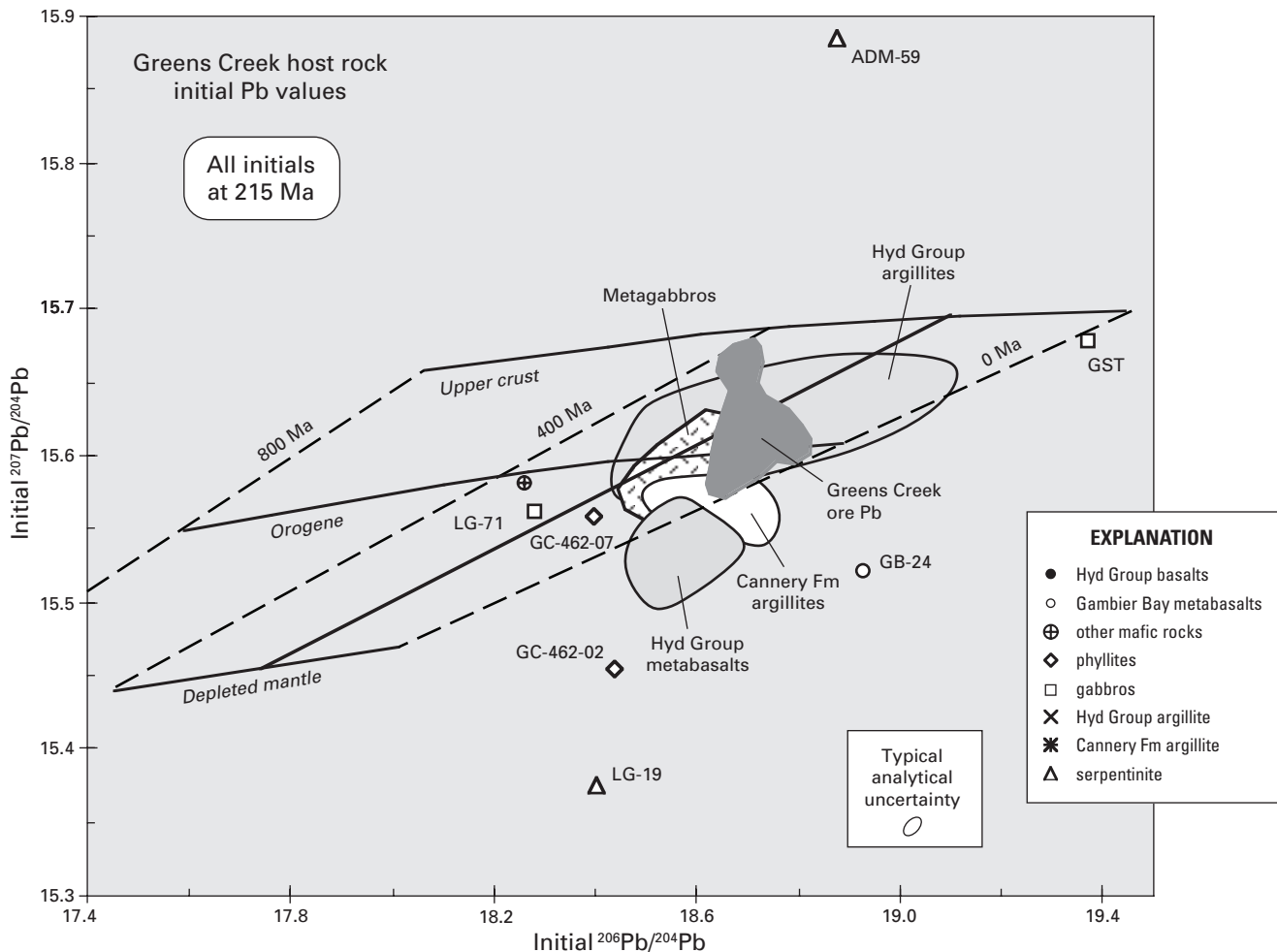


Figure 15. Pb-Pb correlation diagram ($^{206}\text{Pb}/^{204}\text{Pb}$ versus $^{207}\text{Pb}/^{204}\text{Pb}$) showing the distribution of initial lead compositions of Greens Creek host rocks relative to lead isotopic compositions for Greens Creek sulfides (ore). The Greens Creek ore lead compositions ($^{206}\text{Pb}/^{204}\text{Pb} = 18.6 - 18.8$ and $^{207}\text{Pb}/^{204}\text{Pb} = 15.55 - 15.68$) plotted along the “orogene” evolution curve at a model lead age between 0 and 100 Ma. The field for the ore lies within that for the argillites, however, none of the argillite initial lead compositions actually lie on the ore trend, but surround it. Lead isotopic data for Greens Creek ore suggest that it was formed through mixing between two main components: mafic magmatic source(s) represented by compositions of the metabasalts, metagabbros, and serpentinites, and compositions given by the hanging-wall, pyritic, black argillites. See text and chapter 10 for more discussion.

The isotopic data imply that magmatic fluids, emanating from ascending volcanic-arc magmas, mix with overlying marine shales and volcanic sediment. Driven by the heat of the intrusion, hydrothermal circulation of these fluids with high salinity and moderate temperatures through the sediment package, metasomatize the sediment and deposit metals onto the sea floor and into adjacent sediments. The sulfides in this scenario would incorporate the lead isotopic compositions of the magmatic fluid and the marine sediment. This same lead isotopic behavior — ore compositions between basalts and pelagic sediment signatures — has been documented from several modern VMS ore deposits around the world: East Pacific Rise (Dasch and others, 1971; O’Nions and others, 1978; Brevart and others, 1981), Nazca plate MORB (Unruh and Tatsumoto, 1976), Japanese Kuroko deposits (Fehn and others, 1983).

Summary

Initial Pb-Sr-Nd isotopic data indicate a depleted mantle source for Greens Creek host rocks and their associated ore, with very little to no input of any older crustal material. The initial isotopic data scatter somewhat, indicating the likelihood of post-emplacement isotopic disturbances during subsequent metamorphism and(or) alteration by fluid/rock interaction processes. Nonetheless, the isotopic data exhibit elevated $^{206}\text{Pb}/^{204}\text{Pb}$ and $^{87}\text{Sr}/^{86}\text{Sr}$ relative to OIB or MORB trends at 215 Ma and are consistent with isotopic signatures typical of oceanic-arc environments. The Greens Creek host-rock data are similar to other isotopic data from the Alexander and Gravina terranes that support these interpretations.

A sequence of progressively more positive or depleted ϵ_{Nd} and lower $^{87}\text{Sr}/^{86}\text{Sr}$ values throughout the Greens Creek host-rock stratigraphy implies rifting of the preexisting arc crust and emplacement of magmas with progressively higher mantle-derived components. These isotopic data support a genetic model of ore deposition in a rifted oceanic-arc environment.

Lead isotopic values for Greens Creek ore indicate the probability that metals were derived from magmatic fluids emanating from mafic/ultramafic sources and circulating through or mixing with marine shales (argillites).

Acknowledgments

The authors thank the Kennecott Greens Creek Mining Company for their cooperation, hospitality, and special equipment during sample collection on Admiralty Island. Also, thanks to all the workers at the USGS that were responsible for the majority of sample preparation and chemical analysis, especially Elaine Gilman. Special thanks to manuscript reviewers Brian Marshall and Gary Landis for their helpful comments and criticisms. And special thanks to C.D. Taylor and C.A. Johnson, our editors, for having the patience to see this manuscript into review and eventual fruition.

References

- Allegre, C.J., and Luck, J.M., 1980, Osmium isotopes as petrogenetic and geological tracers: *Earth and Planetary Science Letters*, v. 48, p. 148–54.
- Ayuso, R.A., Wooden, J.L., Foley, N.K., Seal, R.R., Sinha, A.K., and Persing, H., 2004, U-Pb zircon ages and Pb isotope geochemistry of gold deposits in the Carolina Slate Belt of South Carolina: *Economic Geology*, v. 100, p. 225–252.
- Barovich, K.M., and Patchett, P.J., 1992, Behavior of isotopic systematics during deformation and metamorphism—A Hf, Nd and Sr isotopic study of mylonitized granite: *Contributions to Mineralogy Petrology*, v. 109, p. 386–393.
- Ben Othman, Dalila, White, W.M., and Patchett, J., 1989, The geochemistry of marine sediments, island arc magma genesis, and crust-mantle recycling: *Earth and Planetary Science Letters*, v. 94, p. 1–21.
- Berg, H.C., Jones, D.L., and Richter, D.H., 1972, Gravina-Nutzotin Belt — Tectonic significance of an upper Mesozoic sedimentary and volcanic sequence in southern and southeastern Alaska: *U.S. Geological Survey Professional Paper 800-D*, p. D1–D24.
- Brevart, Olivier, Dupre, B., and Allegre, C.J., 1981, Metallogenesis at spreading centers — Lead isotope systematics for sulfides, manganese-rich crusts, basalts, and sediments from the Cyamex and Alvin areas (East Pacific Rise): *Economic Geology*, v. 76, p. 1205–1210.
- Burke, W.H., Denison, R.E., Hetherington, E.A., Koepnick, R.B., Nelson, H.F., and Otto, J.B., 1982, Variations of seawater $^{87}\text{Sr}/^{86}\text{Sr}$ throughout Phanerozoic time: *Geology*, v. 10, p. 516–519.
- Dasch, E.J., Dymond, J.R., and Heath, G.R., 1971, Isotopic analysis of metalliferous sediment from the East Pacific Rise: *Earth and Planetary Science Letters*, v. 13, p. 175–180.
- DePaolo, D.J., 1981, Neodymium isotopes in the Colorado Front Range and crust-mantle evolution in the Proterozoic: *Nature*, v. 291, p. 193–196.
- Dickin, Alan, 1995, *Radiogenic isotope geology*: Cambridge, England, Cambridge University Press, 490 p.
- Ellam, R.M., and Hawkesworth, C.J., 1988, Elemental and isotopic variations in subduction related basalts — Evidence for a three component model: *Contributions to Mineralogy and Petrology*, v. 98, pp. 72–80.
- Farmer, G. Lang, Ayuso, R., and Plafker, G., 1993, A Coast Mountains provenance for the Valdez and Orca Groups, southern Alaska, based on Nd, Sr, and Pb isotopic evidence: *Earth and Planetary Science Letters*, v. 116, pp. 9–21.

- Faure, Gunther, 1986, Principles of isotope geology: New York, John Wiley and Sons, 589 p.
- Fehn, Udo, Doe, B.R., and Delevaux, M.H., 1983, The distribution of lead isotopes and the origin of Kuroko ore deposits in the Hokuroku district, Japan: Economic Geology Monograph no. 5, p. 488–506.
- Gaccetta, J.D., and Church, S.E., 1989, Lead isotope data base for sulfide occurrences from Alaska, December, 1989: U.S. Geological Survey Open-File Report 89–688, 60 p.
- Gehrels, G.E., and Berg, H.C., 1992, Geologic map of southeastern Alaska: U.S. Geological Survey Investigation Series Map I–1867, scale 1:600,000.
- Hart, S.R., and Kinloch, E.D., 1989, Osmium isotope systematics in Witwatersrand and Bushveld ore deposits: Economic Geology, v. 84, p. 1651–1655.
- Hawkesworth, C.J., O’Nions, R.K., Pankhurst, R.J., Hamilton, P.J., and Evensen, N.M., 1977, A geochemical study of island-arc and back-arc tholeiites from the Scotia Sea: Earth and Planetary Science Letters, v. 36, pp. 253–262.
- Hawkesworth, C.J., O’Nions, R.K., and Arculus, R.J., 1979, Nd and Sr isotope geochemistry of island arc volcanics, Grenada, Lesser Antilles: Earth and Planetary Science Letters, v. 45, p. 237–248.
- Hess, Jennifer, Bender, M.L., and Schilling, J.G., 1986, Evolution of the ratio of strontium–87 to strontium–86 in seawater from Cretaceous to present: Science, v. 231, p. 979–984.
- Kerrick, Robert, 1991, Radiogenic isotope systems applied to ore deposits, *in* Heaman, L., and Ludden, J.N., eds., Applications of radiogenic isotopes systems to problems in geology, Mineralogical Association of Canada, Short Course 19, p. 365–421.
- Lambert, D.D., Morgan, J.W., Walker, R.J., Shirey, S.B., Carlson, R.W., Zientek, M.L., and Koski, M.S., 1989, Rhenium–osmium and samarium–neodymium isotopic systematics of the Stillwater Complex: Science, v. 244, p. 1169–1174.
- Martin, C.E., 1991, Osmium isotopic characteristics of mantle-derived rocks: Geochimica et Cosmochimica Acta, v. 55, p. 1421–1434.
- Newberry, R.J., and Brew, D.A., 1997, Chemical and isotopic data for rocks and ores from the Upper Triassic Greens Creek and Woewodski Island volcanogenic massive sulfide deposits, southeastern Alaska, *in* Geologic studies in Alaska by the U.S. Geological Survey: U.S. Geological Survey Professional Paper 1614, p. 35–55.
- Newberry, R.J., Brew, D.A., and Crafford, T.C., 1990, Genesis of the Greens Creek volcanogenic massive sulfide deposit, S.E. Alaska — A geochemical study, [abs.]: Geological Association of Canada Program with Abstracts, v. 15, p. A96.
- Newberry, R.J., Crafford, T.C., Newkirk, S.R., Young, L.E., Nelson, S.W., and Duke, N.A., 1997, Volcanogenic massive sulfide deposits of Alaska: Economic Geology Monograph no. 9, p. 120–150.
- O’Nions, R.K., Carter, S.R., Cohen, R.S., Evensen, N.M., and Hamilton, P.J., 1978, Pb, Nd and Sr isotopes in oceanic ferromanganese deposits and ocean floor basalts: Nature, v. 273, p. 435–438.
- Pearce, J.A., 1983, The role of sub-continental lithosphere in magma genesis at destructive plate margins, *in* Hawkesworth, C.J., and Norry, M.J., eds., Continental basalts and mantle xenoliths, p. 230–249: Nantwich, United Kingdom, Shiva Publications, Ltd.
- Premo, W.R., and Tatsumoto, M., 1991, U-Th-Pb isotopic systematics of lunar norite 78235, *in* Proceedings of Lunar and Planetary Science Conference, v. 21, p. 89–100: Houston, Texas, The Lunar and Planetary Institute.
- Premo, W.R., and Tatsumoto, M., 1992, U-Th-Pb, Rb-Sr, and Sm-Nd isotopic systematics of lunar troctolitic cumulate 76535: Implications on the age and origin of this early lunar, deep-seated cumulate, *in* Proceedings of Lunar and Planetary Science Conference, v. 22, p. 381–397: Houston, Texas, The Lunar and Planetary Institute.
- Rubin, C.M., and Saleeby, J.B., 1992, Tectonic history of the eastern edge of the Alexander Terrane, southeast Alaska: Tectonics, v. 11, p. 586–602.
- Rubin, C.M., Saleeby, J.B., Cowan, D.S., Brandon, M.T., and McGroder, M.F., 1990, Regionally extensive mid-Cretaceous west-vergent thrust system in the northwestern Cordillera — Implications for continent-margin tectonism: Geology, v. 18, p. 276–280.
- Samson, S.D., McClelland, W.C., Patchett, P.J., Gehrels, G.E., and Anderson, R.G., 1989, Evidence from neodymium isotopes for mantle contributions to Phanerozoic crustal genesis in the Canadian Cordillera: Nature, v. 337, p. 705–709.
- Samson, S.D., Patchett, P.J., Gehrels, G.E., and Anderson, R.G., 1990, Nd and Sr isotopic characterization of the Wrangellia Terrane and implications for crustal growth of the Canadian Cordillera: Journal of Geology, v. 98, p. 749–762.
- Samson, S.D., Patchett, P.J., McClelland, W.C., and Gehrels, G.E., 1991a, Nd isotopic characterization of metamorphic rocks in the Coast Mountains, Alaskan and Canadian Cordillera — Ancient crust bounded by juvenile terranes: Tectonics, v. 10, p. 770–780.
- Samson, S.D., Patchett, P.J., McClelland, W.C., and Gehrels, G.E., 1991b, Nd and Sr isotopic constraints on the petrogenesis of the west side of the northern Coast Mountains batholith, Alaskan and Canadian Cordillera: Canadian Journal of Earth Science, v. 28, p. 939–946.

- Stacey, J.S., and Kramers, J.D., 1975, Approximation of terrestrial lead isotope evolution by a two stage model: *Earth and Planetary Science Letters*, v. 26, p. 207–221.
- Tatsumoto, Mitsunobu, and Unruh, D.M., 1976, KREEP basalt age — Grain by grain U-Th-Pb systematics study of the quartz monzodiorite clast 15405, 88, *in* Proceedings of the 7th Lunar Science Conference, p. 2107–2129: Houston, Texas, The Lunar Planetary Institute.
- Taylor, C.D., 1997, An arc-flank to back-arc transect — Metallogeny of Late Triassic volcanogenic massive sulfide occurrences of the Alexander terrane, southeastern Alaska and British Columbia: [extended abs.], *in* Society of Economic Geologists Neves Corvo Field Conference, May 7–17, 1997, Lisbon, Portugal, Abstracts and Programs, p. 68.
- Taylor, C.D., Philpotts, J.A., Hall, T.E., and Wakeman, B.W., 1995b, New information on the geochemistry, age, and tectonic history of Late Triassic volcanic host rocks and associated massive sulfide occurrences of the Alexander terrane, southeast Alaska: Alaska Miners Association Conference Juneau, Program with Abstracts, p. 31–32.
- Taylor, C.D., Philpotts, J., Sutley, S., Gent, C., Harlan, S., Premo, W., Tatsumoto, M., Emsbo, P., and Meier, A., 1995a, Geochemistry of late Triassic volcanic rocks and age of alteration associated with volcanogenic massive sulfide occurrences, Alexander terrane, southeast Alaska, *in* *Geology and Ore Deposits of the American Cordillera, A Symposium*, Reno, Nev., 1995: Reno, Nev., Geological Society of Nevada, p. A74.
- Taylor, C.D., Premo, W.R., and Meier, A.L., 1999, The Late Triassic metallogeny of the Alexander terrane, southeastern Alaska and British Columbia: *Geological Society of America Abstracts with Programs*, v. 31, no. 6, p. A–101.
- Taylor, C.D., Premo, W.R., and Lear, K.G., 2000, The Greens Creek massive sulfide deposit — Premier example of the Late Triassic metallogeny of the Alexander terrane, southeastern Alaska and British Columbia: *Geological Society of America Abstracts with Programs*, v. 32, no. 6, p. A–71.
- Unruh, Daniel M., and Tatsumoto, M., 1976, Lead isotopic composition and uranium, thorium and lead concentrations in sediments and basalts from the Nazca plate: Initial Report of Deep Sea Drilling Project, v. 34, p. 341–347.
- Walker, R.J., Morgan, J.W., Naldrett, A.J., and Li C., 1991, Re-Os isotopic systematics of Ni-Cu sulfide ores, Sudbury Igneous Complex, Ontario — Evidence for a major crustal component: *Earth and Planetary Science Letters*, v. 105, p. 416–429.
- Whitehouse, M.J., 1988, Granulite facies Nd-isotopic homogenization in the Lewisian complex of northwest Scotland: *Nature*, v. 331, p. 705–707.
- Zartman, R.E., 1984, Lead, strontium, and neodymium isotopic characterization of mineral deposits relative to their geologic environments, *in* Proceedings of the 27th International Geological Congress, Moscow, v. 12, p. 83–106, *Metallogenesis and mineral ore deposits: Utrecht, The Netherlands*, VNU Science Press.
- Zartman, R.E., and Doe, B.R., 1981, Plumbotectonics — The model: *Tectonophysics*, v. 75, p. 135–162.